Efimov effect in the Born-Oppenheimer picture

Hamidreza Saberbaghi*

November 21, 2025

Abstract

In this work, we study the Efimov effect in a mass-imbalanced system consisting of two heavy particles and one light particle within the Born–Oppenheimer approximation. The result obtained in [23] for zero angular momentum is recovered here as a special case, and the analysis is extended to all angular momenta.

In this setting, the resonant heavy–light interactions are modeled as point interactions, under the assumption of either exchange symmetry or antisymmetry with respect to the positions of the delta centers. Within this framework, we prove that in the unitary limit the Efimov spectrum depends solely on the mass ratio and particle statistics; that is, the so-called three-body parameter is absent. We also provide a condition ensuring that the spectrum contains no non-Efimov eigenvalues. Furthermore, we study the system away from the unitary limit and show that the spatial size of the weakest bound state near the threshold is approximately 2.8 times the two-body scattering length, in contrast to the common assumption that these two scales coincide. Finally, we compute Bargmann's bound for the number of bound states and obtain a sharper estimate than the results in the literature.

Keywords: Efimov effect, Born-Oppenheimer approximation, Stationary Scattering theory, Point interactions

*University of Insubria, Science and High Technology Department, Via Valleggio 11, 22100 Como, Italy.
Email: `hamidreza.saberbaghi@uninsubria.it`

1 Introduction

1.1 Background

The Efimov effect [16, 17] is the low-energy phenomenon in the spectrum of the Hamiltonian of a three-body system in $\mathbb{R}^3$. At low energies, the range of the inter-particle forces becomes negligible compared to the de Broglie wavelength of the particles. Therefore, the behavior of quantum systems and specifically its scattering properties exhibits a *universal* characteristic largely independent of the specifics of the short-range interactions [8]. The defining parameter of such systems is the two-body S-wave scattering length, determined as the zero-energy limit of the scattering amplitude:

$$a := \lim_{|k|\to 0} f\left(k, k'\right) . \tag{1.1}$$

Here, $f(k, k')$ denotes the scattering amplitude in three dimensions and a denotes the two-body scattering length.

In a three particle system, Efimov effect arises if at least two of the three possible pairs of particles engage in *zero-energy resonance*. Zero-energy resonance refers to a two-body interaction that does not support a bound state and its energy is at the bottom of the continuous spectrum. Equivalently, this state characterized by *unitary limit*, *i.e.*, infinite two-body scattering length. Under these assumptions, although the individual two-body subsystems are not bound, there exist infinitely many shallow three-body bound states E_n with relatively large spatial sizes, accumulating at zero energy, *i.e.*, $E_n \to 0$. Moreover, the ratio of successive binding energies of these states follows to the universal geometric scaling law described by:

$$\lim_{n\to\infty} \frac{E_n}{E_{n+1}} = \mathrm{e}^{\frac{2\pi}{s}} , \tag{1.2}$$

where s is a dimensionless parameter that depends on the number of resonant pairs, the mass ratio of the particles, and their statistics.

Since the Efimov effect is independent of the details of short-range interactions, zero-range potentials (also known as Fermi pseudo-potentials [20, 9]) provide a natural framework for studying this problem. However, the presence of the so-called "Thomas effect" or "fall of the particles to the center" [49, 35, 34] makes the Hamiltonian of the three-body system with zero-range forces unstable, *i.e.*, there exists a sequence of energy eigenvalues unbounded from below. To avoid this ultraviolet divergence, Efimov formally worked with short-ranged potentials with the range $r_0 > 0$. Using hyperspherical coordinates (see, for example, [36, Sec. 6.2]), he reduced the Schrödinger operator to an equation for the hyper-angle together with an effective radial equation for the function $F_s(R)$:

$$-\frac{1}{2m_0}\left(\frac{\mathrm{d}^2}{\mathrm{d}R^2} + \frac{1}{R}\frac{\mathrm{d}}{\mathrm{d}R} - \frac{s^2}{R^2}\right) F_s(R) = E\, F_s(R). \tag{1.3}$$

Here, R is the hyperradius, s is the parameter appearing in (1.2) and is determined by the corresponding hyperangular equation, m_0 denotes the reduced mass (which depends on the number of resonant pairs), and E is the energy eigenvalue.

Efimov regarded equation (1.3) as the description of the long-range interaction, *i.e.*, it is valid for $R \geq R_0$, which $R_0 \gg r_0$. He then argued that, at R_0, one can match the short-range solution (obtained, for example, from a sharp momentum cutoff) with the long-range solution provided by (1.3), and, in this way, obtain the eigenvalues:

$$E_n = -\frac{1}{2m_0\, R_0^2}\, \mathrm{e}^{-2\pi n/|s|} \exp \frac{2}{|s|} \left[\arctan \frac{\varLambda R_0}{|s|} - \varDelta \right] . \tag{1.4}$$

Here, $\varLambda$ is a parameter that contains information about the short-range interaction[1], and $\varDelta$ is a phase used to match the solution at R_0.

In fact, the idea of introducing a "three-body parameter" that fixes a physical observable, and thereby obtain a momentum cutoff (or more generally, a boundary condition) is well known in the physics literature (see, *e.g.*, [30] and also [36] for the further discussion and references). In particular, the three-body parameter determines the solution of the Schrödinger operator on the interval $[0, R_0]$.

Furthermore, it is straightforward to verify that the geometrical law (1.2) follows from (1.4). More recently, Efimov's idea has been given a rigorous mathematical formulation by Fermi, Ferretti, and Teta [19], who imposed a hard-core potential at the origin to avoid the Thomas effect.

In mathematical physics literature of Efimov effect, various authors studied the logarithmic growth of the number of eigenvalues, as the three-body energy converges to zero (see *e.g.* [52, 47, 48, 6]). Also, Efimov suggested that the number of eigenvalues is proportional to $\ln \frac{a}{r_0}$, given the energy is sufficiently low.

Moreover, Efimov studied three-body systems with various mass ratios and particle statistics. In particular, he examined the case of two heavy particles and one light particle, where the resonant interaction occurs only between the light particle and each of the heavy ones [17, Sec. 5.2]. He considered this configuration the most favorable for the appearance of the Efimov effect, since the scaling factor $\mathrm{e}^{2\pi/s}$ in (1.2) decreases as the mass ratio increases. (For three identical bosons, the parameter s is close to 1.)

Let us introduce the three-body Hamiltonian associated to this mass-imbalanced case. The particles interact through a general two-body potential V. Consider two identical heavy particles of mass M located at positions $y_i \in \mathbb{R}^3$ for $i = 1, 2$, and a light particle of mass m at position $y_3 \in \mathbb{R}^3$. The Hamiltonian acts on a Hilbert space with either bosonic or fermionic symmetry, denoted by L^2_b and L^2_f, respectively. These are subspaces of $L^2(\mathbb{R}^9)$ consisting of square-integrable functions that are symmetric or anti-symmetric under the exchange of y_1 and y_2:

$$\begin{aligned} L^2_b(\mathbb{R}^9) &:= \{\varPsi \in L^2(\mathbb{R}^9) \mid \varPsi(y_1, y_2, y_3) = \varPsi(y_2, y_1, y_3)\}, \\ L^2_f(\mathbb{R}^9) &:= \{\varPsi \in L^2(\mathbb{R}^9) \mid \varPsi(y_1, y_2, y_3) = -\varPsi(y_2, y_1, y_3)\}. \end{aligned} \tag{1.5}$$

Denoting the Hamiltonian with bosonic (resp. fermionic) symmetry by $\mathcal{H}^b_{2+1}$ (resp. $\mathcal{H}^f_{2+1}$), we define

$$\mathcal{H}^{b/f}_{2+1} := -\frac{\hbar^2}{2M} (\varDelta_{y_1} + \varDelta_{y_2}) - \frac{\hbar^2}{2m} \varDelta_{y_3} + \mu V(y_3 - y_1) + \mu V(y_3 - y_2), \tag{1.6}$$

[1] Efimov defined it as the logarithmic derivative of the interior solution at R_0, which he claimed is a constant and determined by the momentum cutoff.

where, μ is a coupling constant. For simplicity, we also set $\hbar^2 = 1$.
Introducing the Jacobi coordinates, the center of mass, and the effective mass parameter γ,

$$x = y_3 - \tfrac{1}{2}(y_1 + y_2), \quad R = y_1 - y_2, \quad x_{\mathrm{cm}} = \frac{M(y_1 + y_2) + my_3}{2M + m}, \quad \gamma = \frac{2Mm}{2M + m}. \tag{1.7}$$

We may (with a slight abuse of notation, using the same symbol) rewrite the Hamiltonian in Jacobi coordinates as

$$\mathcal{H}^{b/f}_{2+1} = -\frac{1}{2(2M + m)}\varDelta_{x_{\mathrm{cm}}} - \frac{1}{M}\varDelta_R - \frac{1}{2\gamma}\varDelta_x + \mu V(x - R/2) + \mu V(x + R/2). \tag{1.8}$$

The bosonic (resp. fermionic) symmetry in (1.5) then translates into

$$\varPsi(x_{\mathrm{cm}}, x, R) = \varPsi(x_{\mathrm{cm}}, x, -R) \quad (\text{resp. } \varPsi(x_{\mathrm{cm}}, x, R) = -\varPsi(x_{\mathrm{cm}}, x, -R)).$$

Without loss of generality, we set the coupling constant $\mu = \frac{1}{2\gamma}$. (In the limit $M \to \infty$, this coefficient approaches 1, since $\gamma \to 1$.) Neglecting the center-of-mass contribution and introducing the parameter $\varepsilon^2 = \frac{2\gamma}{M}$, we obtain the rescaled Hamiltonian

$$\mathcal{H}^{b/f}_{\varepsilon} := -\varepsilon^2 \varDelta_R - \varDelta_x + V(x - R/2) + V(x + R/2), . \tag{1.9}$$

Because of the intrinsic complexity of the three-body problem, any rigorous treatment of the ultraviolet divergence is highly technical (see, *e.g.*, [5, 28, 21]). This motivates the use of the Born–Oppenheimer approximation, a standard approach in the study of molecular systems.[2] In this framework, the three-body problem is reduced to an effective one-body problem in the presence of two fixed scattering centers.

1.2 Born-Oppenheimer approximation

We now introduce the Born–Oppenheimer approximation in the zero-range framework at a formal level and recall some earlier results. For background on the history of this method and related developments, we refer to the review by Jecko [29], which also provides a comprehensive list of references.

We assume that the two-body interaction V in (1.9) is given by a zero-range potential, formally represented by δ.

As mentioned earlier, in the Born–Oppenheimer approximation the heavy particles are treated as stationary relative to the motion of the light particle. Accordingly, the total wave function can be factorized as

$$\varPsi(x, R) = \psi(x; R)\, \varPhi(R)$$

[2] Efimov himself suggested this idea in his original paper, where he considered the limit of an infinite mass ratio between the heavy and light particles [17].

Treating R as a parameter, we solve the eigenvalue problem for the light particle:

$$\mathcal{H}_x, \psi(x;R) := [-\Delta_x + \delta(x+R/2) + \delta(x-R/2)]\,\psi(x;R) = V_{\text{eff}}(|R|)\,\psi(x;R)\,. \tag{1.10}$$

Setting $r := |R|$, we replace the corresponding terms of $\mathcal{H}_x$ in (1.9) with its eigenvalue $V_{\text{eff}}(r)$ as an effective potential. This reduces the three-body Hamiltonian to an effective one-dimensional problem:

$$\mathcal{H}_{\text{eff}}\,\Phi(R) := \left[-\varepsilon^2 \Delta_R + V_{\text{eff}}(r)\right]\Phi(R) = E^{\text{eff}}\,\Phi(R),. \tag{1.11}$$

In the Born–Oppenheimer picture, the energy E^{eff} serves as an approximation to the three-body energy of the Hamiltonian $\mathcal{H}_\varepsilon^{b/f}$ in (1.9).

To study this problem in a mathematically rigorous way, one must first characterize the formal Hamiltonian (1.10) in order to determine $V_{\text{eff}}(r)$. Subsequently, one can solve the eigenvalue problem (1.11) to obtain E^{eff}. Finally, one should compare the three-body energy in (1.9) with E^{eff} and compute the error of this approximation, rigorously. In this paper, we address only the first two questions and comment on the validity of this approach in the conclusion.

There are numerous studies of the Born–Oppenheimer approximation for the $2+1$ mass-imbalanced particle system in Efimov physics (see, *e.g.*, [25, 26] for the pioneering works, and [18, 51, 44] for later contributions). In [25], Fonseca, Redish, and Shanley considered a two-body potential V of the Yamaguchi form [53]. Within this framework, they demonstrated the occurrence of the Efimov effect in the unitary limit $a \to \infty$. Furthermore, they computed semiclassical bounds for the number of bound states, such as Bargmann's and Calogero's bounds, and showed that these bounds depend logarithmically on the two-body scattering length a away from the unitary limit.

The Yamaguchi separable potential used in [25, 26] serves as a formal approximation of a point interaction. However, it is well known that if one considers *local* point interactions, a sub-family of point interactions, as the two-body potentials in the light-particle Hamiltonian (1.10), the resulting effective Hamiltonian (1.11) becomes unstable. More precisely, when the distance between the two scattering centers tends to zero, one finds $V_{\text{eff}}(r) = O(\frac{1}{r^2})$ as $r \to 0$, which gives rise to a sequence of eigenvalues diverging to $-\infty$. (see (2.17) below.)

In [23], we addressed this issue by characterizing the full family of self-adjoint extensions of the operator $\dot{\mathcal{H}}_0 = -\Delta \restriction C_0^\infty(\mathbb{R}^3 \setminus y_1, y_2)$ for the special case of spinless particles, under the assumption of exchange symmetry of the scattering centers. This assumption means that, under the transformation $R \to -R$ in (1.10), the wave function of the light particle remains unchanged, *i.e.*, it is a suitable regime for describing bosonic symmetry.

In the present work, we extend these results to the antisymmetric exchange, that is, the fermionic case, and analyze the Hamiltonian (1.11) for higher angular momenta. We show that, within the Born–Oppenheimer picture, in contrast to (1.4), the Efimov spectrum is independent of the details of short-range interactions, as expected in a zero-range model. Moreover, we study the spectrum of (1.11) away from the unitary limit and improve upon existing results in this regime.

1.3 Main results and plan of the paper

In Section 2, we analyze the Hamiltonian of the light particle given in (1.10). As mentioned earlier, a detailed construction of this Hamiltonian under the assumption of exchange symmetry was presented in [23]. For completeness, we briefly recall the main steps of that construction and extend it to the antisymmetric case.

We then obtain the eigenvalue of the Hamiltonian (1.10) (or equivalently, the effective potential of the Hamiltonian (1.11)) in the unitary limit, which has the form

$$V_{\text{eff}}(r) = -\lambda_1(r) = -\frac{1}{r^2}\left[W\left(\mathrm{e}^{g_\theta(r)}\right) - g_\theta(r)\right]^2, \quad g_\theta(r) = \mathrm{e}^{-r/\sqrt{2}}\left(\sin\tfrac{r}{\sqrt{2}} + \cos\tfrac{r}{\sqrt{2}}\right), \tag{1.12}$$

where $W(x)$ denotes the Lambert function (see [11]).

We conclude the section with a discussion of the physical relevance of the model introduced here.

In Section 3, we study the eigenvalue problem (1.11) both in and away from the unitary limit. Let l denote the angular momentum. Under suitable conditions on the mass ratio (see Lemma 3.2 below), we establish the following result in the unitary limit:

Theorem 1.1. *There exists an infinite sequence of negative eigenvalues E_n^{eff} of the effective Hamiltonian* (1.11) *with the effective potential* (1.12)*, such that $E_n^{\text{eff}} \to 0$ for $n \to \infty$. Moreover,*

$$E_n^{\text{eff}} = -\varepsilon^2 \frac{32}{9\pi^2}\, e^{\frac{2}{\beta}\left(\arctan\left(\frac{2\beta}{2l+1}\right) + \phi_\beta - n\pi\right)}\left(1 + \zeta_n\right) \tag{1.13}$$

where $\beta = \sqrt{-l(l+1) + \varepsilon^{-2}\, W(1)^2 - 1/4}$, $\phi_\beta = \arg\Gamma(1 + i\beta)$ and $\zeta_n \to 0\,,$ for $n \to \infty$.

Also, we provide a sufficient condition that E_1^{eff} in (1.13) is the ground state of the system; equivalently, the spectrum contains no non-Efimov eigenvalues.

We continue with a discussion of the spectrum of (1.11) away from the unitary limit. We estimate the spatial size $\mathcal{S}$ of the weakest near-threshold state as $\mathcal{S} \simeq 2.80\, a_\theta(0)$, contrary to the common guess $\mathcal{S} = a$ (see *e.g.*, [17, 25, 36]), where a is the two-body scattering length. Moreover, we compute Bargmann's semi-classical estimate for the number of eigenvalues and obtain a sharper bound than in [25]. We conclude with a qualitative description of how the spectrum deforms away from unitarity: the near-threshold states are only Efimov-like and no longer satisfy the geometrical law (1.2). Some of the results also reported in [45].

2 Hamiltonian of the light particle

In this section we introduce the Hamiltonian of the light particle, associated with the formal expression (1.10). We discussed characterization of such a Hamiltonian in details with symmetry exchange assumption in [23, 45]. For the sake of completeness, here we briefly review it and extend this construction to the anti-symmetry exchange as well.

We follow closely the von Neumann theory of the self-adjoint extensions of

$$\dot{\mathcal{H}}_0 = -\Delta \restriction C_0^\infty(\mathbb{R}^3 \setminus \{y_1, y_2\})\,,$$

studied by Dabrowski and Gross in [13] with some changes on notations. Note that they did not assume any symmetry assumptions on the scattering centers and characterize the set of all self-adjoint extensions in $\mathbb{R}^d$, $d = 1, 2, 3$ and for any finite number of the centers.

In the physics literature, the Hamiltonian of the light particle (1.10) often characterized by Bethe-Peierls boundary conditions [7] on the scattering centers, where the Hamiltonian acts as a free Hamiltonian on the whole space $\mathbb{R}^3$ but the points $\{y_1, y_2\}$. This formal description can be made rigorous (see Remark 2.4 below). From a mathematical perspective, however, it is more convenient to construct the operator via von Neumann's extension theory, starting from $\dot{\mathcal{H}}_0$ and classifying its self-adjoint extensions through the deficiency spaces.

Let us denote the defect spaces of $\dot{\mathcal{H}}_0$ and its adjoint respectively by $N_{\pm i}$ and $\mathcal{H}^\dagger$. A defect space N_z of the densely defined symmetric operator $\dot{\mathcal{H}}_0$ is defined as $\ker\left(\mathcal{H}^\dagger - \bar{z}\right)$ for any $z \in \mathbb{C} \setminus \mathbb{R}^+$. A closed symmetric operator has self-adjoint extensions if and only if the dimensions of the defect spaces are equal (see *e.g.*, [41, section X.1, p. 141]). In the case of $\dot{\mathcal{H}}_0$, N_i and N_{-i} are both two-dimensional. Moreover, these extensions parametrized by the unitary operators

$$J : N_{+i} \to N_{-i}\,.$$

Setting $G_{\pm i}$ as the fundamental solution (Green's function) of Helmholtz equation, *i.e.* $(-\Delta \mp i)G^n_{\pm i} = \delta_{y_n}$, $n = 1, 2$ in $\mathbb{R}^3$. In fact, they are eigenfunctions of $\mathcal{H}^\dagger$ relative to the eigenvalues $\pm i$ and explicitly written as:

$$G^n_{\pm i}(x\,; y_n) = \frac{e^{i\sqrt{\pm i}|x-y_n|}}{4\pi|x-y_n|}, \quad n = 1, 2, \quad x \in \mathbb{R}^3\,.$$

Any function in the domain of of a self-adjoint extension of $\dot{\mathcal{H}}_0$ is a combination of $H^2(\mathbb{R}^3)$ function (*i.e.*, domain of the free Laplacian) and bases of defect spaces. Without any symmetry assumptions on scattering centers, the defect spaces characterized as:

$$N_{\pm i} = \left\{ f \in L^2(\mathbb{R}^3) \,|\, f = c_1 G^1_{\pm i} + c_2 G^2_{\pm i} \right\}, \quad c_1, c_2 \in \mathbb{C}\,. \tag{2.1}$$

Moreover, a unitary map J between defect spaces act on bases of the defect spaces via a 2×2 matrix U:

$$JG^m_i = \sum_{n=1}^{2} U_{nm}\, c_n G^n_{-i}$$

Furthermore, we assume:

- the scattering centers are identical. This means the matrix U is constrained to be diagonal, with each diagonal element expressed as $e^{i\theta}$, where $0 \le \theta < 2\pi$;
- the wave function of the light particle under the exchange the positions of the centers, either remains unchanged or flips its sign. The symmetry (resp. anti-symmetry) assumption means $c_1 = c_2$ (resp. $c_1 = -c_2$) in (2.1).

Henceforth, for the sake of simplicity, we choose $c_1, c_2 \in \{1, -1\}$. Let us denote self-adjoint extensions of $\dot{\mathcal{H}}_0$ by $\mathcal{H}_\theta$. Also, we define matrix function S:

$$S_{mn}(\bar{z},w) = \langle \overline{c_m G_z^m}\,, c_n G_w^n \rangle, \quad z, w \in \mathbb{C}, \quad 1 \le m, n \le 2,$$

where $\langle\, ,\, \rangle$ denotes the scalar product in $L^2(\mathbb{R}^3)$. With these preparations, we can apply Krien's formula and obtain the resolvent of $\mathcal{H}_\theta^{b/f}$:

$$\left(\mathcal{H}_\theta^{b/f} - z\right)^{-1} = G_z + \sum_{m,n=1}^{2} \left[\mathit{\Gamma}_\theta^{b/f}(z)^{-1}\right]_{mn} \left(\overline{G_z(\cdot - y_m)}, \cdot\right) G_z(\cdot - y_n)\,, \tag{2.2}$$

where the matrix $\mathit{\Gamma}_\theta(z)$ is defined as:

$$\mathit{\Gamma}_\theta^{b/f}(z) = 2iS(i,i)(U^T + I)^{-1} - (z+i)S(\bar{z}, -i).$$

It is easy to see that $2i(U^T + I)^{-1}$ forms a diagonal matrix, with each diagonal element being $t_\theta := (1 + \tan\frac{\theta}{2})$. The parameter $-\infty < t_\theta < \infty$ labels the self-adjoint extensions and closely related to the scattering length of the system (see (2.12) below). Setting

$$z = \bar{z} = -\lambda,\ \lambda \in \mathbb{R}^+\,,$$

a straightforward computation (see [23, eq. 16]) shows that:

$$[\mathit{\Gamma}_\theta^b(-\lambda)]_{kj} = \left[\frac{\sqrt{\lambda}}{4\pi} + \frac{t_\theta - 1}{4\sqrt{2}\pi}\right]\delta_{kj} + \left[\frac{1}{4\pi r}\left(\mathrm{e}^{-r/\sqrt{2}}(t_\theta \sin\frac{r}{\sqrt{2}} + \cos\frac{r}{\sqrt{2}}) - \mathrm{e}^{-\sqrt{\lambda}r}\right)\right](1 - \delta_{kj})\,, \tag{2.3}$$

and

$$[\mathit{\Gamma}_\theta^f(-\lambda)]_{kj} = \left[\frac{\sqrt{\lambda}}{4\pi} + \frac{t_\theta - 1}{4\sqrt{2}\pi}\right]\delta_{kj} - \left[\frac{1}{4\pi r}\left(\mathrm{e}^{-r/\sqrt{2}}(t_\theta \sin\frac{r}{\sqrt{2}} + \cos\frac{r}{\sqrt{2}}) - \mathrm{e}^{-\sqrt{\lambda}r}\right)\right](1 - \delta_{kj})\,. \tag{2.4}$$

Unlike local point interactions, the Hamiltonian $\mathcal{H}_\theta^{b/f}$ does not develop singularities as the distance between two scattering centers tends to zero. In fact, in the bosonic case, as $r \to 0$, the resolvent (2.2) of $\mathcal{H}_\theta^b$, which describes an evolution of a free particle interacting with two identical centers that can exchange their positions, converges in the strong resolvent sense (*i.e.*, in the point-wise topology) to the resolvent of a one-center point interaction. In the fermionic case, as $r \to 0$, the resolvent (2.2) of $\mathcal{H}_\theta^f$ converges to the free resolvent, which is consistent with the Pauli principle.
Moreover, the equation $\det \mathit{\Gamma}_\theta^{b/f}(-\lambda) = 0$ determines the eigenvalue $-\lambda$ of the light-particle Hamiltonian, which serve as the effective potential $V_{\text{eff}}(r)$ in (1.11). We summarize these observations in the following proposition. The proof for the symmetry exchange case was given in [23, Lemma 3.1], while the fermionic case is analogous and is therefore omitted.

Proposition 2.1. *For a fixed* $t_\theta \le 1$,

- Case (i): Symmetry exchange.

1. *If $r \to 0$, the resolvent (2.2) of $\mathcal{H}^b_\theta$ converges in the strong resolvent sense to the resolvent of a one-center point interaction with integral kernel*

$$G_\lambda f + \frac{4\pi}{\sqrt{\lambda} + \frac{t_\theta - 1}{\sqrt{2}}}\, \overline{G_\lambda f(y)}\, G_\lambda(\cdot - y). \tag{2.5}$$

2. *The operator $\mathcal{H}^b_\theta$ has two eigenvalues, given as the solutions of the equation* $\det \Gamma^b_\theta(-\lambda) = 0$. *They correspond to the eigenfunctions*

$$G_\lambda(x - y_1) + G_\lambda(x - y_2) \quad \text{and} \quad G_\lambda(x - y_1) - G_\lambda(x - y_2),$$

respectively. The associated eigenvalues in the implicit form are

$$\begin{aligned} \mathrm{e}^{-\sqrt{\lambda}\, r} - \sqrt{\lambda}\, r + \tfrac{r}{\sqrt{2}}\,(1 - t_\theta) - g_\theta(r) = 0, \\ -\mathrm{e}^{-\sqrt{\lambda}\, r} - \sqrt{\lambda}\, r + \tfrac{r}{\sqrt{2}}\,(1 - t_\theta) - h_\theta(r) = 0, \end{aligned}$$

where

$$\begin{aligned} g_\theta(r) &:= +\mathrm{e}^{-r/\sqrt{2}} \left(t_\theta \sin \tfrac{r}{\sqrt{2}} + \cos \tfrac{r}{\sqrt{2}} \right) \\ h_\theta(r) &:= -\mathrm{e}^{-r/\sqrt{2}} \left(t_\theta \sin \tfrac{r}{\sqrt{2}} + \cos \tfrac{r}{\sqrt{2}} \right). \end{aligned} \tag{2.6}$$

3. *For $k \in \mathbb{R}^3$, generalized eigenfunctions of $\mathcal{H}^b_\theta$ characterized as:*

$$\Psi^b_{\theta, y_1, y_2}(k, x) = e^{ik\cdot x} + \sum_{m,n=1}^{2} \left[\Gamma^b_\theta(|k|^2) \right]^{-1}_{mn} e^{ik\cdot y_n} \frac{e^{i|k||x - y_m|}}{4\pi |x - y_m|}, \qquad k \in \mathbb{R}^3, x \in \mathbb{R}^3 \setminus \{y_1, y_2\}. \tag{2.7}$$

- *Case (ii): anti-symmetry exchange.*

1. *If $r \to 0$, the resolvent (2.2) of $\mathcal{H}^f_\theta$ converges in the strong resolvent sense to the free resolvent.*

2. *The operator $\mathcal{H}^f_\theta$ has two eigenvalues, given as the solutions of the equation* $\det \Gamma^f_\theta(-\lambda) = 0$. *They correspond to the eigenfunctions*

$$G_\lambda(x - y_1) + G_\lambda(x - y_2) \quad \text{and} \quad G_\lambda(x - y_1) - G_\lambda(x - y_2),$$

respectively. The associated eigenvalues in the implicit form are

$$\begin{aligned} -\mathrm{e}^{-\sqrt{\lambda}\, r} - \sqrt{\lambda}\, r + \tfrac{r}{\sqrt{2}}\,(1 - t_\theta) - h_\theta(r) = 0\,, \\ \mathrm{e}^{-\sqrt{\lambda}\, r} - \sqrt{\lambda}\, r + \tfrac{r}{\sqrt{2}}\,(1 - t_\theta) - g_\theta(r) = 0\,, \end{aligned}$$

where $g_\theta(r)$ and $h_\theta(r)$ defined in (2.6).

3. For $k \in \mathbb{R}^3$, generalized eigenfunctions of $\mathcal{H}_\theta^f$ characterized as:

$$\Psi^f_{\theta,y_1,y_2}(k,x) = \mathrm{e}^{ik\cdot x} + \sum_{m,n=1}^{2} (-1)^{m+n} \left[\Gamma^f_\theta(|k|^2)\right]^{-1}_{mn} \mathrm{e}^{ik\cdot y_n} \frac{\mathrm{e}^{i|k||x-y_m|}}{4\pi|x-y_m|}, \qquad k \in \mathbb{R}^3\,, x \in \mathbb{R}^3\backslash\{y_1,y_2\}\,. \tag{2.8}$$

Let us briefly comment on the above proposition.

- The family $\mathcal{H}_\theta^{b/f}$ is a rank-two perturbation of the free Laplacian. Therefore, the strong resolvent convergence in the limit $r \to 0$ cannot improved to norm–resolvent convergence (see *e.g.* [40, Theorem VIII.23]).
- Imposing antisymmetry under exchange of the scattering centers, replaces $\Gamma^b_\theta(-\lambda)$ by $\Gamma^f_\theta(-\lambda)$, which differs only by a sign in the off-diagonal entries. In either symmetry case, only one eigenvalue equation is compatible with the symmetry, namely

  $$\mathrm{e}^{-\sqrt{\lambda}\,r} - \sqrt{\lambda}\,r + \tfrac{r}{\sqrt{2}}\,(1-t_\theta) - g_\theta(r) = 0\,. \tag{2.9}$$

  The corresponding eigenfunction is proportional to $G_\lambda(x-y_1) + G_\lambda(x-y_2)$ (resp. $G_\lambda(x-y_1) - G_\lambda(x-y_2)$) in the bosonic (resp. fermionic) case. Moreover, in (2.8) there is an extra factor $(-1)^{m+n}$ compared to (2.7). This sign is precisely what enforces antisymmetry under exchange of the scattering centers, *i.e.*, contributions associated with indices of opposite parity (*i.e.*, $m+n$ odd) pick up a minus sign. Additionally, both in the bosonic and fermionic cases, away from the centers, the generalized eigenfunctions satisfy

  $$-\Delta\,\Psi^{b/f}_{\theta,y_1,y_2}(k,x) = k^2\,\Psi^{b/f}_{\theta,y_1,y_2}(k,x), \qquad k \in \mathbb{R}^3,\ x \in \mathbb{R}^3 \setminus \{y_1,y_2\}\,.$$

  We also recall that generalized eigenfunctions of $\mathcal{H}_\theta^{b/f}$ are not square-integrable,

  $$\Psi^{b/f}_{\theta,y_1,y_2}(k,x) \notin L^2(\mathbb{R}^3),$$

  and they represent the continuous part of the spectrum; see, *e.g.*, [43].

By characterizing the generalized eigenfunctions of $\mathcal{H}_\theta^{b/f}$, we can compute the (on-shell) scattering amplitude and, in particular, the scattering length. Note that the standard two-body scattering length is defined for a single, radial potential and represents the *effective length* that characterizes how the potential acts on a free quantum particle in low energies.
In the present two-center setting, the interaction is neither radial nor reducible to a single two-body channel; nevertheless, the scattering amplitude is well defined (see [3, Section II.2.5]). For $\omega,\omega' \in S^2$

and $k \geq 0$:

$$
\begin{aligned}
f_{\theta,y_1,y_2}\left(k,\omega,\omega'\right) &= \lim_{\substack{|x|\to\infty \\ x/|x|=\omega}} |x|\mathrm{e}^{-ik|x|}\left[\Psi^{b/f}_{\theta,y_1,y_2}\left(k\omega',x\right) - \mathrm{e}^{ik\omega'\cdot x}\right] \\
&= \frac{1}{4\pi}\sum_{m,n=1}^{2}\left[\Gamma^{b}_{\theta}\left(k^2\right)\right]^{-1}_{mn}\mathrm{e}^{ik(y_m\omega'-y_n\omega)} \\
&= \frac{1}{4\pi}\sum_{m,n=1}^{2}(-1)^{m+n}\left[\Gamma^{f}_{\theta}\left(k^2\right)\right]^{-1}_{mn}\mathrm{e}^{ik(y_m\omega'-y_n\omega)}\,.
\end{aligned}
\tag{2.10}
$$

The scattering length of $\mathcal{H}^{b/f}_{\theta}$ is then defined as the zero-energy limit of the scattering amplitude. To distinguish it from the two-body scattering length a in (1.1), we denote it by $a_\theta(r)$ and set:

$$
a_\theta(r) := -\lim_{k\to 0} f_{\theta,y_1,y_2}\left(k,\omega,\omega'\right)\,. \tag{2.11}
$$

Corollary 2.2. *For fixed t_θ, the scattering length $a_\theta(r)$ of $\mathcal{H}^{b/f}_{\theta}$ defined in* (2.11) *explicitly computed as:*

$$
a_\theta(r) = \frac{-1}{4\pi}\lim_{k\to 0}\sum_{m,n=1}^{2}\left[\Gamma^{b}_{\theta}(k)^{-1}\right]_{mn} = \frac{-1}{4\pi}\lim_{k\to 0}\sum_{m,n=1}^{2}(-1)^{m+n}\left[\Gamma^{f}_{\theta}(k)^{-1}\right]_{mn} = \frac{2r}{\frac{r}{\sqrt{2}}\left(1-t_\theta\right)-g_\theta(r)+1}\,,
$$

where $g_\theta(r)$ defined in (2.6)*. In particular:*

$$
a_\theta(r) = \begin{cases} \frac{2\sqrt{2}}{1-t_\theta} & \text{for} \quad r\to+\infty \\ \frac{\sqrt{2}}{1-t_\theta} & \text{for} \quad r\to 0\,, \end{cases} \tag{2.12}
$$

so, $a_\theta(r)$ diverges like $(1-t_\theta)^{-1}$ as $t_\theta\to 1$ (the unitary limit).

The asymptotics of the scattering length $a_\theta(r)$ for $r\to 0$ and $r\to\infty$ are consistent with the physical picture of two centers that, respectively, merge into a single scatterer or decouple at large separation. This confirms the physical relevance of the self-adjoint extensions parametrized by t_θ. To support this further, we examine the eigenvalue equation (2.9), recalling that $-\lambda(r)$ plays the role of the effective potential in the Born–Oppenheimer equation (1.11).

The implicit equation (2.9) can be solved explicitly in terms of the Lambert W-function. Set $s := \sqrt{\lambda}\,r$ and

$$
A(r) := \frac{r}{\sqrt{2}}\left(1-t_\theta\right) - g_\theta(r)\,,
$$

where $g_\theta(r)$ was introduced in (2.6). Then, (2.9) is equivalent to

$$
\mathrm{e}^{-s} = s - A(r)\,, \qquad \Longleftrightarrow \qquad \big(s-A(r)\big)\,\mathrm{e}^{\,s-A(r)} = \mathrm{e}^{-A(r)}\,.
$$

By definition of Lambert W as the inverse of $x\mapsto x\,\mathrm{e}^{x}$,

$$
s - A(r) = W\big(\mathrm{e}^{-A(r)}\big)\,, \qquad \text{hence} \qquad \sqrt{\lambda}\,r = A(r) + W\big(\mathrm{e}^{-A(r)}\big).
$$

Therefore,

$$V_{\text{eff}}(r) = -\lambda_\theta(r) = -\frac{1}{r^2}\left[W\left(\mathrm{e}^{-\frac{r}{\sqrt{2}}(1-t_\theta)+g_\theta(r)}\right) - \left(-\tfrac{r}{\sqrt{2}}\left(1-t_\theta\right)+g_\theta(r)\right)\right]^2, \quad t_\theta \le 1\,, \tag{2.13}$$

Since $\mathrm{e}^{-A(r)} > 0$ for real $A(r)$, the right-hand side involves the principal real branch W, smooth on $(-\mathrm{e}^{-1}, \infty)$. This representation will be useful below for extracting asymptotics and regularity properties of $-\lambda_\theta(r)$. Note that for $t_\theta > 1$, The spectrum of $\mathcal{H}_\theta^{b/f}$, only consists of the essential spectrum.
The eigenvalue $-\lambda_\theta(r)$ in (2.13) has an interesting long-range behavior in the unitary limit $t_\theta = 1$; $-\lambda_\theta(r) \to -\frac{W^2(1)}{r^2}$. This inverse-squared behavior is the essence of Efimov effect. Henceforth, we set $\lambda_1(r) := \lambda_\theta(r), \;\; t_\theta = 1$.
Moreover, $g_\theta(r)$ is an oscillatory function that damps exponentially fast with the roots at

$$r_k = \sqrt{2}\left(-\cot^{-1}(t_\theta) + k\pi\right), \quad k \in \mathbb{N},\, 0 \le t_\theta \le 1\,,$$

and

$$r_k = \sqrt{2}\left(-\cot^{-1}(t_\theta) + (k-1)\pi\right), \quad k \in \mathbb{N},\, t_\theta < 0\,.$$

Here, we defined

$$\cot^{-1}(t_\theta) : (-\infty, 0) \cup (0, \infty) \to (-\pi/2, 0) \cup (0, \pi/2)\,,$$

with $\cot^{-1}(0) := \frac{\pi}{2}$.
Furthermore, $-\lambda_\theta(r)$ in (2.13) is analytic. The principal branch $W_0(x)$ has a Taylor expansion about $x = 0$ with radius e^{-1} (Corless et al. [11]). In the next section, we need to estimate $-\lambda_\theta(r)$ in and away from the unitary limit. The following lemma states analyticity of $-\lambda_\theta(r)$ and provides the required estimates; the proof is given in Appendix A.

Lemma 2.3. *The function $-\lambda_\theta(r)$ defined in* (2.13) *is analytic for $r > 0$. Furthermore, for $t_\theta = 1$, we have*

$$-\lambda_1(r) = \begin{cases} -\dfrac{W^2(1)}{r^2} + O\big(\mathrm{e}^{-r/\sqrt{2}}\big) & \textit{for} \quad r \to +\infty \\ -\dfrac{r^2}{16} + O\big(r^3\big) & \textit{for} \quad r \to 0\,, \end{cases} \tag{2.14}$$

and the radius of convergence of its Taylor series about the point $r = 0$ is infinite to the right. Also, for $t_\theta < 1$,

$$-\lambda_\theta(r) = \begin{cases} -\dfrac{(1-t_\theta)^2}{2} + O\Big(\dfrac{\mathrm{e}^{-r/\sqrt{2}}}{r}\Big) & \textit{for} \quad r \to +\infty \\ -\dfrac{(1-t_\theta)^2}{2} + O(r) & \textit{for} \quad r \to 0\,. \end{cases} \tag{2.15}$$

and the radius of convergence of its Taylor series about the point $r = a_\theta(0)$ is infinite to the right, where $a_\theta(0)$ was computed in (2.12).

It is instructive to compare the properties of $\mathcal{H}_\theta^{b/f}$ with two-center *local* point interactions. For $n > 1$, n-center local point interactions are subfamily of point interactions that constructed based on the physical intuition of one-center problem, *i.e.*, as a collection n one-center subsystems. They are parametrized by $\alpha := -\frac{1}{4\pi a}$, where a is the two-body scattering length (1.1). We denote such a Hamiltonian by $\mathcal{H}^{b/f}_{\underline{\alpha}}$, with the superscript indicating the symmetry (bosonic/fermionic) under exchange of the centers. The bosonic two-center case $\mathcal{H}^{b}_{\underline{\alpha}}$ is treated in [3, Chapter II.1, p. 119]. One obtains the resolvent of $\mathcal{H}^{b}_{\underline{\alpha}}$ by replacing $\Gamma^b_\theta(-\lambda)$ in (2.3) with

$$[\Gamma^b_{\underline{\alpha}}(-\lambda)]_{kj} = \left[\frac{\sqrt{\lambda}}{4\pi} + \alpha\right]\delta_{kj} + \left[-\mathrm{e}^{-\sqrt{\lambda}r}\right](1-\delta_{kj})\,. \tag{2.16}$$

where $r = |y_1 - y_2|$. Hence, the eigenvalue associated with the symmetric eigenfunction $G_\lambda(x-y_1) + G_\lambda(x-y_2)$ solves as:

$$-\lambda_{\text{local}} = -\frac{1}{r^2}\left[W\left(\mathrm{e}^{4\pi\alpha r}\right) - (4\pi\alpha r)\right]^2, \quad \alpha \le 0\,. \tag{2.17}$$

We observe that regardless of the value of $\alpha \le 0$,

$$\lim_{r\to 0}\big(-\lambda_{\text{local}}(r)\big) = -\frac{W^2(1)}{r^2}\,.$$

This produces an inverse-square singularity strong enough to cause a similar effect to so-called fall-to-the-center in the effective Hamiltonian (1.11) if one sets $V_{\text{eff}} = -\lambda_{\text{local}}(r)$. For $\alpha = 0$ (the unitary limit, since then $a = \infty$), (2.17) yields an inverse-squared law $-\lambda_{\text{local}}(r) = -\frac{W(1)^2}{r^2}$ for any reason $r > 0$. Figure 1 compares (2.13) for $t_\theta = 1$ with (2.17) for $\alpha = 0$.

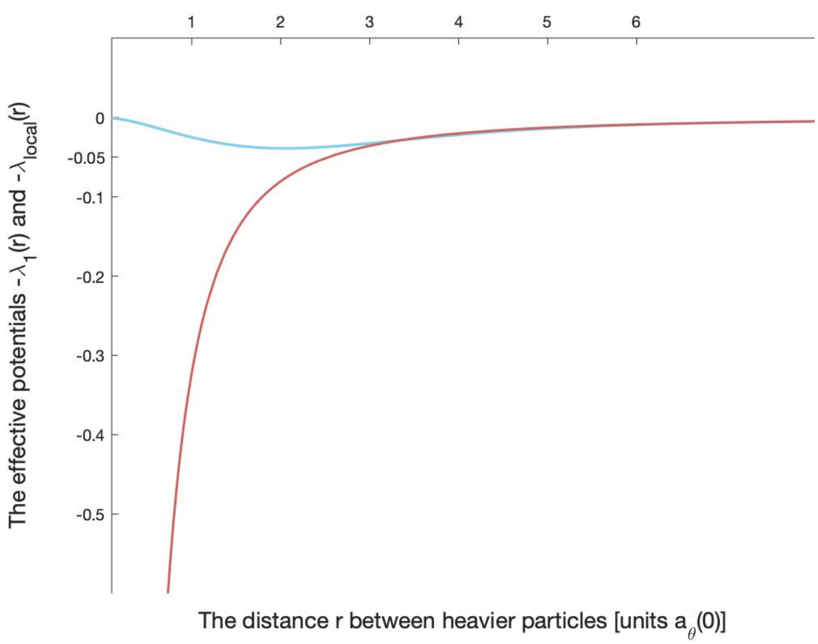

Figure 1: The light blue line represents $-\lambda_1(r)$ and the red line represents $-\lambda_{\text{local}} = \frac{-W^2(1)}{r^2}$ for $\alpha = 0$. The two curves intersect for $r_k = \sqrt{2}(\frac{3\pi}{4} + k\pi)$, $k - 1 \in \mathbb{N}$ and apart from an exponentially decreasing oscillation they coincide for $r > r_0$.

Furthermore, if one computes the (two–center) scattering length $a_{\underline{\alpha}}(r)$ for $\mathcal{H}^{b}_{\underline{\alpha}}$ (which is not a two–body quantity and should be defined analogously to Corollary 2.2; see [3, Section II.1.5]), one finds

$$\lim_{r\to 0} a_{\underline{\alpha}}(r) = 0.$$

In the same limit the resolvent of $\mathcal{H}^b_{\underline{\alpha}}$ converges to the free resolvent in the strong resolvent sense. Thus, as the distance between the two delta centers shrinks to zero, the pair effectively disappears, while the corresponding eigenvalue of the system diverges to $-\infty$.

The case $\mathcal{H}^f_{\underline{\alpha}}$ (anti–symmetric exchange of the centers) is analogous: $\Gamma^f_{\underline{\alpha}}$ is obtained by flipping the sign of the off–diagonal terms in (2.16); the relevant eigenvalue is still given by (2.17), and again $a_{\underline{\alpha}}(r) \to 0$ as $r \to 0$ (with the resolvent converging to the free one in the strong resolvent sense).

Remark 2.4. In light of the discussion above, it is natural to relate $\mathcal{H}^b_\theta$ to $\mathcal{H}^b_{\underline{\alpha}}$ (and similarly for the fermionic case) by connecting their expansion parameters via

$$\alpha = \frac{t_\theta - 1}{4\sqrt{2}\,\pi}.$$

With this identification, (2.3) can be rewritten as:

$$[\Gamma^{b/f}_\theta(-\lambda)]_{kj} = \left[\tfrac{\sqrt{\lambda}}{4\pi} + \alpha\right]\delta_{kj} \;\pm\; \left[\tfrac{1}{4\pi r}\big(g_\theta(r) - \mathrm{e}^{-\sqrt{\lambda}\,r}\big)\right](1-\delta_{kj})\,, \tag{2.18}$$

where $+$ (resp. $-$) corresponds to exchange symmetry (resp. exchange anti–symmetry), and $g_\theta(r)$ is defined in (2.6). The only difference from the matrix (2.16) is the appearance of $g_\theta(r)$ in the off–diagonal entries. Moreover, one can formulate Bethe–Peierls–type boundary conditions at each center. For $q \in \mathbb{C}$, in the symmetry–exchange case,

$$\psi^b(x) = q\left(\frac{1}{4\pi|x-y_i|} + \alpha + g_\theta(r)\right) + O(1), \qquad i = 1,2, \quad |x-y_i| \to 0. \tag{2.19}$$

In the anti–symmetry–exchange case,

$$\psi^f(x) = (-1)^{i+1} q\left(\frac{1}{4\pi|x-y_i|} + \alpha + h_\theta(r)\right) + O(1), \qquad i = 1,2, \quad |x-y_i| \to 0, \tag{2.20}$$

where $h_\theta(r)$ is defined in (2.6). Unlike in the local point–interaction model (where g_θ and h_θ are absent), the singular boundary conditions (2.19)–(2.20) remain well defined as $r \to 0$.

It is worth noting that various authors have proposed different procedures to renormalize the singularities in (2.16) (see, *e.g.*, [32, 2, 22]). In particular, Ferretti and Teta replace g_θ in (2.18) with a function $\theta(r)$ satisfying $\theta'(0) = 0$ [22, Proposition 4.2].

This raises a natural question: which model is physically relevant? We address this issue by comparing the results of Proposition 2.1, Corollary 2.2, and Remark 2.4 with standard physical expectations.

We expect that when the two heavy particles are far apart, the light particle localizes near one of the centers, so the three-body system reduces to a dimer plus a free particle, unless it is at the unitary limit. In the Born–Oppenheimer picture, this implies that the scattering length of the Hamiltonian

(1.10) at $r \to \infty$ should be twice its value at $r \to 0$: at large separation the free particle has two binding options, whereas in the $r \to 0$ limit the two centers act as a single center. This expectation is precisely aligned with (2.12).

Moreover, when the trimer reduces to a dimer and a free particle as $r \to \infty$, the energy should coincide with the dimer bound-state energy, which obeys the universal relation

$$E = -\frac{1}{a^2} = -(4\pi\alpha)^2,$$

where a is the two-body scattering length from (1.1) and α is the extension parameter of the one-center point interaction [3, Theorem I.1.4]. Using the asymptotics of $-\lambda_\theta(r)$ in (2.15) together with the identification $\alpha = \frac{t_\theta - 1}{4\sqrt{2}\pi}$, we see that $\mathcal{H}_\theta^{b/f}$ satisfies this requirement. Likewise, in the opposite two-body limit $r \to 0$, $\mathcal{H}_\theta^b$ converges to a single-center point interaction that again yields $E = -1/a^2 = -(4\pi\alpha)^2$ (see (2.5)).

Interestingly, the family of point interactions introduced here can (formally) be viewed as the zero-range limit of the short-range two-body potentials employed by Fonseca *et al.* [26, 25]. [3]

Furthermore, as discussed in the introduction, when the two-body potentials in (1.9), and hence in (1.10), are taken in the zero-range limit, one naturally expects that no additional three-body parameter (such as Λ in (1.4)) enters the Efimov spectrum. In our setting, the condition

$$-\lambda_1(0) = \lim_{r\to\infty} \big(-\lambda_1(r) \big) = 0$$

plays a crucial role in the proof of Theorem 1.1 (see Lemma 3.6 and Remark 3.7). Recall that the Efimov effect arises when at least two of the three possible two-body subsystems are at zero-energy resonance. Heuristically, the requirement $-\lambda_1(0) = \lim_{r\to\infty}(-\lambda_1(r)) = 0$ is the mathematical encoding of this scenario: at the unitary limit ($t_\theta = 1$), the eigenvalue of $\mathcal{H}_\theta^{b/f}$ vanishes in both limits $r \to 0$ and $r \to \infty$.

We conclude this chapter with a remark on the relation between $a_\theta(r)$, the scattering length associated with $\mathcal{H}_\theta^{b/f}$, and the two-body scattering length a in (1.1).

[3](We warn the reader that the notation used in this footnote is similar to that employed in the work of Fonseca *et al.* [25] and is specific to this footnote, bearing no relevance to the current work.) In [25], the authors defined the two-body potential taken to be $V = \lambda \left| g \right\rangle \left\langle g \right|$, where λ is the coupling constant, given by $\lambda^{-1} = \langle g| (\epsilon_0 + \nabla^2/\nu') |g\rangle$. Here, ϵ_0 represents the two-body light-heavy bound state, $\nu' = \frac{M}{M+m}$ is a mass ratio, and $|g\rangle$ is a Yamaguchi-type state with $\langle p|\, g\rangle = (p^2+\beta^2)^{-1}$ for a momentum p. The parameter β is a non-zero constant (and often considered as the range of the potential).
For the two-body zero-energy resonance in the unitary limit, *i.e.* $\epsilon_0 = 0$, one obtains $\lambda_c = \frac{\beta^3}{\nu'\pi^2}$, where λ_c denotes the value of λ in the unitary limit. In other words, there is no heavy-light bound state with a magnitude less than the critical value of the coupling constant λ_c. Denoting $\kappa_0^2 := -\nu'\epsilon_0$ and $\kappa^2(|R|) := -\nu'\epsilon(|R|)$, the effective potential $\epsilon(|R|)$ tends to this pair-wise bound state $-\frac{\epsilon_0}{\nu}$ as $|R| \to \infty$. As a result, in the very large distances between two heavier particles, *i.e.* $\kappa_0|R| >> 1$, the light particle becomes localized on one of the heavy particles. Furthermore, it is a regular potential at the origin, *i.e.* we have $\kappa(0) = (\sqrt{2}-1)\beta + \kappa_0$.
Therefore, we expect at zero-range limit (if the limit exists), *i.e.*, $\beta \to 0$, the effective potential $\epsilon(|R|)$ has the same value at $R = 0$ and at $R \to \infty$.

Remark 2.5. As noted earlier, $-\lambda_\theta(0) = -(1/a_\theta(0))^2$; however,

$$-\lim_{r\to\infty} \lambda_\theta(r) \;\neq\; -\lim_{r\to\infty} \big(1/a_\theta(r)\big)^2.$$

Moreover, at $t_\theta = 1$ we have $a_\theta(0) = \lim_{r\to\infty} a_\theta(r) = \infty$, while for any fixed $r > 0$ one still has $a_\theta(r) < \infty$ (see Corollary 2.2). Thus, $a_\theta(r)$, $r > 0$, is a distance-dependent scattering length for the two-center problem and should not be confused with the two-body scattering length a.
On the other hand, as discussed in Remark 2.4, identifying

$$\alpha = \frac{t_\theta - 1}{4\sqrt{2}\pi}$$

gives

$$a_\theta(0) = -\frac{1}{4\pi\alpha},$$

so $a_\theta(0)$ coincides with the usual two-body scattering length associated with a single-center point interaction. For this reason we still use the term *unitary limit* for $t_\theta = 1$ (*i.e.*, $\alpha = 0$), even though $a_\theta(r)$ itself refers to scattering of a free particle against two centers.

3 The spectrum of the effective Hamiltonian

In this section we study the eigenvalues of the Hamiltonian $\mathcal{H}_{\text{eff}}$ in (1.11), where the effective potential $V_{\text{eff}}(r)$ is given by (2.13). Recall that

$$\mathcal{H}_{\text{eff}} \;:=\; -\varepsilon^2 \Delta_R \;+\; V_{\text{eff}}(r), \qquad D(\mathcal{H}_{\text{eff}}) = \{\, \Phi \in H^2(\mathbb{R}^3) \,\}.$$

By the Kato–Rellich theorem the operator is self-adjoint (see, *e.g.*, [42]). Moreover, using (2.14) and (2.15), we see that

$$\sigma_{\text{ess}}(\mathcal{H}_{\text{eff}}) = \Big[-\tfrac{(1-t_\theta)^2}{2},\, \infty\Big),$$

and any discrete eigenvalues satisfy

$$\sigma_{\text{p}}(\mathcal{H}_{\text{eff}}) \subset \big[\min V_{\text{eff}},\, -\tfrac{(1-t_\theta)^2}{2}\big).$$

Furthermore, since the potential $V_{\text{eff}}(r)$ is radial, $D(\mathcal{H}_{\text{eff}})$ is invariant under rotations, and we may apply the partial-wave expansion. Fixing the angular momentum $l \geq 0$, we decompose $\Phi \in L^2(\mathbb{R}^3)$ into a radial part $r^{-1}u(r) \in L^2(\mathbb{R}^+; r^2\,\mathrm{d}r)$ and spherical harmonics $Y_{lm}(\phi, \theta) \in L^2(S^2; \mathrm{d}\Omega)$, where S^2 is the unit sphere in $\mathbb{R}^3$ with surface measure $\mathrm{d}\Omega$. Applying the unitary map $L^2(\mathbb{R}^+; r^2\,\mathrm{d}r) \to L^2(\mathbb{R}^+; \mathrm{d}r)$ given by $f \mapsto rf$ yields the radial equation for $u(r)$:

$$\begin{gathered} -\varepsilon^2 \left(u''(r) - \frac{l(l+1)}{r^2} u(r) \right) + V_{\text{eff}}(r) u(r) = E^{\text{eff}} u(r), \\ u \in L^2(\mathbb{R}^+), \quad \lim_{r\to 0} u(r) = 0, \quad \lim_{r\to 0} r^{-(l+1)} u(r) = 1 \end{gathered} \tag{3.1}$$

where $u(r) = r\Phi$ (see [41, Appendix to X.1, Example 4], [43, Theorem XI.53], [42, Ch. XIII.3.B]). In general, (3.1) is understood as a differential operator acting on $L^2(\mathbb{R}^+)$. However, since the effective potential is analytic (see Lemma 2.3), any solution of (3.1) is smooth. Henceforth, we focus our analysis on the Hamiltonian (3.1).

In the first part of this section, we analyze the spectrum of (3.1) at the unitary limit $t_\theta = 1$, where $a_\theta(0) \to \infty$ and $V_{\text{eff}}(r) = -\lambda_1(r)$ as in (2.13), with asymptotic behavior given by (2.14). We prove Theorem 1.1 in several steps. We then provide a sufficient condition, depending only on the mass ratio, ensuring that the ground state of (3.1) is the first Efimov eigenvalue.

In the second part, we trace the Efimov spectrum away from the unitary limit. We first estimate the spatial size of the weakest Efimov-like eigenvalue, then compute Bargmann's bound and show its logarithmic dependence on the scattering length. We conclude with a qualitative description of the spectrum.

3.1 Efimov effect in the unitary limit

Recall that in the unitary limit $t_\theta = 1$ the effective potential reads

$$V_{\text{eff}}(r) = -\lambda_1(r) = -\frac{1}{r^2}\left[W\left(\mathrm{e}^{g_\theta(r)}\right) - g_\theta(r)\right]^2, \qquad g_\theta(r) = \mathrm{e}^{-r/\sqrt{2}}\left(\sin\tfrac{r}{\sqrt{2}} + \cos\tfrac{r}{\sqrt{2}}\right).$$

Moreover, $r_k = \sqrt{2}\left(\frac{3\pi}{4} + k\pi\right)$, $k - 1 \in \mathbb{N}$, are the roots of $g_\theta(r)$ for $t_\theta = 1$. For $r > r_0$, $-\lambda_1(r)$ is well approximated by $-\frac{W(1)^2}{r^2}$, up to an exponentially decaying oscillation. This observation motivates us to introduce a family of operators $\mathcal{H}_k$, $k - 1 \in \mathbb{N}$:

$$\mathcal{H}_k := -\varepsilon^2 \Delta + V_k\,, \qquad D(\mathcal{H}_k) = H^2(\mathbb{R}^3)\,, \tag{3.2}$$

where

$$V_k(r) = \begin{cases} -\lambda_1(r) & \text{if } 0 \le r \le r_k, \\ -\dfrac{W^2(1)}{r^2} & \text{if } r > r_k. \end{cases} \tag{3.3}$$

It is straightforward to check (see [23, proof of Theorem 4.4]):

Lemma 3.1. *The family of operators $\mathcal{H}_k$ converges in the norm resolvent sense to $\mathcal{H}_{\text{eff}}$ as $k \to \infty$.*

Consequently, once the Efimov effect is proved for $\mathcal{H}_k$, $k - 1 \in \mathbb{N}$, it extends to the Hamiltonian $\mathcal{H}_{\text{eff}}$ by Lemma 3.1. It is also well-known that the one-dimensional radial problem

$$-u''(r) - \frac{\mu}{r^2} u = 0 \tag{3.4}$$

has infinitely many eigenvalues accumulating at zero if and only if $\mu > \frac{1}{4}$ (see, *e.g.*, [46, Sec. 4.6]). This threshold arises from using the modified Bessel function K with purely imaginary index as the long-range solution of (3.1) (see the proof of Proposition 3.3 below). In addition, for any angular momentum $l \ge 1$, (3.1) contains the repulsive centrifugal term $\varepsilon^2 \frac{l(l+1)}{r^2}$, which competes with the attractive part of $V_k(r)$. The next lemma gives the corresponding mass-threshold condition.

Lemma 3.2. *For fixed $l-1 \in \mathbb{N}$, the problem* (3.1) *with effective potential V_{eff} of the form* (3.3) *has infinitely many eigenvalues, if and only if $\frac{M}{m} \geq \mathcal{M}_l^*$, where*

$$\mathcal{M}_l^* = \frac{4l(l+1)+1-W(1)^2}{2W(1)^2} \,. \tag{3.5}$$

Proof. Recall that $\varepsilon^2 = \frac{2\gamma}{M}$ with $\gamma = \frac{2Mm}{2M+m}$. Substituting these into the condition (3.4) for (3.1) and calculating the effective inverse-square coefficient yields (3.5). □

It is worth noting that the value in (3.5) is close to that obtained from a direct three-body analysis in hyperspherical coordinates. For example, for $l=1$ one finds $\mathcal{M}_1^* \simeq 13.4902$, to be compared with the critical mass 13.6069 reported via the hyperspherical method (see, *e.g.*, [36, Sec. 6.2.4] and references therein).

The next step is to prove the Efimov effect for (3.1) with an effective potential of the form

$$V_{\text{aux}}(r) = \begin{cases} \Lambda & \text{if } 0 \leq r \leq r_0, \\ -\dfrac{W^2(1)}{r^2} & \text{if } r > r_0, \end{cases} \tag{3.6}$$

where $\Lambda \leq 0$ is a constant and $r_0 > 0$ is arbitrary. We also rescale the energy in (3.1) by setting

$$\begin{aligned} E^{\text{eff}} &= -\varepsilon^2\eta^2, \qquad \eta > 0, \\ \xi &= \sqrt{\eta^2 + \varepsilon^{-2}\Lambda}\, r_0 \,. \end{aligned} \tag{3.7}$$

A special case of Proposition 3.3 (with $\Lambda = 0$ and $l = 0$) was proved in [23, Prop. 4.1]. The present proof follows a similar strategy and is given in Appendix B. We then extend Proposition 3.3 to the potentials (3.3), in particular to V_0 with $r_0 = \sqrt{2}\,\frac{3\pi}{4}$.

Proposition 3.3. *For the problem* (3.1) *with the potential* (3.6)*, there exists an infinite sequence of negative eigenvalues E_n^{eff} such that $E_n^{\text{eff}} \to 0$ as $n \to \infty$. Moreover,*

$$E_n^{\text{eff}} = -\varepsilon^2 \frac{4}{r_0^2}\, e^{\frac{2}{\beta}\left(\arctan\left(2\beta f(\xi_0)\right) + \phi_\beta - n\pi\right)} \left(1 + \zeta_n\right), \tag{3.8}$$

where $\beta = \sqrt{-l(l+1) + \varepsilon^{-2}W(1)^2 - 1/4}$, $\phi_\beta = \arg \Gamma(1+i\beta)$, $\zeta_n \to 0$, for $n \to \infty$, $\xi_0 = \sqrt{\varepsilon^2\Lambda}\, r_0$, and

$$f(\xi_0) := \frac{I_{l+1/2}(\xi_0)}{2\xi_0\, I'_{l+1/2}(\xi_0)} \,,$$

where I is the modified Bessel function of the first kind. In particular, for $\Lambda = 0$ in (3.6)*,*

$$\lim_{\xi_0 \to 0} f(\xi_0) = \frac{1}{2l+1} \,.$$

Corollary 3.4. *For any $\Lambda \le 0$, the eigenvalue formula* (3.8) *yields the Efimov geometric law*

$$\lim_{n\to\infty} \frac{E_n^{\mathrm{eff}}}{E_{n+1}^{\mathrm{eff}}} = \mathrm{e}^{\frac{2\pi}{\beta}}\,. \tag{3.9}$$

Remark 3.5. We can also characterize the eigenfunctions for (3.1) with the potential (3.6). Recall that (3.1) was derived from (1.11) by setting $u(r) = r\,\Phi$. Using the solutions (B.7) in the proof of the proposition, the eigenfunction corresponding to E_n^{eff} can be written as

$$\psi_n(r) = \begin{cases} D\,\dfrac{\sqrt{r_0}\,K_{i\beta}(\eta_n r_0)}{(\sqrt{\varepsilon^{-2}|E_n^{\mathrm{eff}}|+\Lambda}\,r_0)^{\frac{1}{2}}\,I_{l+1/2}(\sqrt{\varepsilon^{-2}|E_n^{\mathrm{eff}}|+\Lambda}\,r_0)}\,\dfrac{(\sqrt{\varepsilon^{-2}|E_n^{\mathrm{eff}}|+\Lambda}\,r)^{\frac{1}{2}}\,I_{l+1/2}(\sqrt{\varepsilon^{-2}|E_n^{\mathrm{eff}}|+\Lambda}\,r)}{r}\,, & r < r_0 \\ D\,\dfrac{K_{i\beta}(\sqrt{\varepsilon^{-2}|E_n^{\mathrm{eff}}|})}{\sqrt{r}}\,, & r > r_0 \end{cases} \tag{3.10}$$

where D is a normalization constant.

The final step before proving Theorem 1.1 is to extend the eigenvalue formula (3.8) with $\Lambda = 0$ to the problem (3.1) with the effective potential of the form (3.3). Intuitively, because the Efimov binding energies in (3.8) are low, we expect the short-range behavior of the potential does not affect the wave function, provided the condition (B.9) for $f(\tau_0)$ holds. In fact, the value of the effective potential at the origin, $V_{\mathrm{eff}}(0)$, plays a crucial role in ensuring this condition.

In [23] we used an ad-hoc argument to prove Lemma 3.6 for the special case $l = 0$. Let $r_{\min}$ denote the point where $-\lambda_1(r)$ attains its minimum. That proof relied heavily on the positivity of $-\lambda_1'(r)$ on $(r_{\min}, r_0]$. For $l > 0$, however, the repulsive centrifugal term competes with $-\lambda_1$, and the quantity $\left(\frac{-2l(l+1)}{r^3} - \varepsilon^{-2}\lambda_1'(r)\right)$ is not guaranteed to be positive, even under the mass-ratio condition (3.5). We therefore adopt a different approach.

Our main tool is Ulam stability for second-order ordinary differential equations (see, *e.g.*, [4, 12]). We follow [4] with some notational changes. Define a second-order differential operator $\mathcal{D}$ on $C^2(I,\mathbb{R})$ by

$$\mathcal{D}(f) := a(r)f''(r) + b(r)f'(r) + c(r)f(r) - d(r)\,, \tag{3.11}$$

where a, b, c, d are at least continuous on I. We say that $\mathcal{D}$ is Ulam stable on I if there exists a constant C such that, for every $\delta > 0$ and every $h \in C^2(I,\mathbb{R})$ satisfying

$$\sup_{r\in I} \left|a(r)h''(r) + b(r)h'(r) + c(r)h(r) - d(r)\right| \le \delta\,, \tag{3.12}$$

there is a C^2 solution $f(r)$ of (3.11) with

$$\sup_{r\in I} \left|h(r) - f(r)\right| \le C\delta\,. \tag{3.13}$$

To prove (3.13), one typically derives the Riccati equation associated with (3.11):

$$a(r)\left(\rho'(r) + \rho^2(r)\right) + b(r)\rho(r) = 0\,. \tag{3.14}$$

Let $I=(\gamma,\sigma)$ and define:

$$\kappa_1(r) := \int_r^\sigma \frac{\mathrm{e}^{\int_r^\sigma \left(\rho(t)+\frac{b(t)}{a(t)}\right)\mathrm{d}t}}{|a(s)|}\mathrm{d}s, \qquad \kappa_2(r) := \int_\gamma^r \mathrm{e}^{\int_s^r \rho(t)\mathrm{d}t}\mathrm{d}s\,. \tag{3.15}$$

If $\|\kappa_i\|_\infty < \infty$, $i=1,2$, then (3.11) is Ulam stable on I (see [4, Theorem 3.1, (ii)]).
We apply Ulam stability to compare solutions of (3.1) with the auxiliary potential (3.6) and with $V_{\text{eff}} = V_k$ in (3.3). We must exclude a neighborhood of the origin $r=0$, where the associated Riccati equation is not well-defined, and treat that interval separately.

Lemma 3.6. *Let $f(r)$ (resp. $f_0(r)$) denote the solution of* (3.1) *with effective potential $V_{\text{eff}} = V_k$ in* (3.3) *(resp. $V_{\text{eff}} = V_{\text{aux}}$ in* (3.6)*). Then, for any $l \geq 0$, on the interval $[0, r_k]$ with $r_k = \sqrt{2}(\frac{3\pi}{4}+k\pi)$, $k-1\in\mathbb{N}$, there exists a constant $C_k > 0$ such that*

$$\big|f(r) - f_0(r)\big| \leq C_k\,(\eta r)^{l+1} \tag{3.16}$$

Proof. Recall the equation (3.1) and boundary conditions:

$$-\varepsilon^2\left(u''(r) - \frac{l(l+1)}{r^2}u(r)\right) + V_{\text{eff}}(r)u(r) = E^{\text{eff}}u(r),$$
$$u\in L^2(\mathbb{R}^+), \quad \lim_{r\to 0} u(r) = 0, \quad \lim_{r\to 0} r^{-(l+1)}u(r) = 1$$

Scale the energy as $-\varepsilon^2\eta^2$. Let $V_k^{-1}(\eta^2)$ be the point where $V_k(r)+\eta^2 = 0$. We split $[0,r_k]$ into $[0, V_k^{-1}(\eta^2)]$ and $(V_k^{-1}(\eta^2), r_k]$ and analyze (3.1) on them separately.

- ***step 1*: *the interval* $[\mathbf{0}, \mathbf{V_k^{-1}}(\eta^2)]$:**
  Since $-\lambda_1(r)$ is analytic and bounded, $-\lambda_1(r)\in L^1\cap L^\infty$ on the interval $[0, V_k^{-1}(\eta^2)]$. Therefore, we can write $f(r)$ as the solution of (3.1) with with the effective of potential $V_{\text{eff}} = V_k$ in (3.3) on this interval as (see *e.g.* [37]):

$$f(r) = f_0(r) + \big(f_0 * (-\lambda_1\cdot f)\big)(r)\,, \tag{3.17}$$

  where the convolution $\big(f_0 * (-\lambda_1\cdot f)\big)(r)$ defined as

$$\int_0^r -\lambda_1(t)f(t)\,f_0(r-t)\mathrm{d}t, \quad t>0\,.$$

  From the proof of Proposition 3.3, $f_0(r) = A\sqrt{\eta r}I_{l+1/2}(\eta r)$, with $I_{l+1/2}$ the modified Bessel function of the first kind and $A\in\mathbb{C}$. Set $\tau = \eta r$. As $\tau\to 0$,

$$\sqrt{\tau}I_{l+1/2}(\tau) = \frac{1}{2l+1}\sqrt{\frac{2}{\pi}}\,\tau^{l+1} + O(\tau^{l+3})\,. \tag{3.18}$$

  Without loss of generality take $A\in\mathbb{R}^+$. Then, by (B.1), $f_0, f_0', f_0'' > 0$ on $[0, V_k^{-1}(\eta^2)]$. On this interval $\eta^2 + V_k^{-1}(\eta^2) \geq 0$ by definition, so similarly $f, f', f'' > 0$. Hence $\big(f_0 * (-\lambda_1\cdot f)\big) < 0$, which implies $|f_0(r)| \geq |f(r)|$ on $[0, V_k^{-1}(\eta^2)]$. Moreover, for $\tau\to 0$, (3.18) yields

$$\int_0^{V_k^{-1}(\eta^2)} -\lambda_1(t) f(t)\, f_0(r-t)\mathrm{d}t \le L_1\, \tau^{l+1}\,, \tag{3.19}$$

where the constant

$$L_1 = V_k^{-1}(\eta^2) \sup_{r\in[0,V_k^{-1}(\eta^2)]} \left|\lambda_1(r)f(r)\right|.$$

- ***step 2: the interval*** $(\mathbf{V_k^{-1}}(\eta^{\mathbf{2}}), \mathbf{r_k}]$**:**
  Here we apply Ulam stability directly. Substituting (3.1) into (3.11) with $E = -\varepsilon^2\eta^2$ gives

  $$a(r) = 1, \quad b(r) = 0, \quad c(r) = \varepsilon^{-2}\lambda_1(r) - \frac{l(l+1)}{r^2} - \eta^2, \quad d(r) = 0\,.$$

  Since we have excluded $r = 0$, $c(r)$ is not singular. From Lemma 2.3, $-\lambda_1(r)$ is analytic and the radius of convergence of its Taylor series about the origin is infinite. This fact, implies that by the Cauchy–Kovalevskaya theorem (see, *e.g.*, [27]), the solution $f(r)$ is unique and analytic on $(V_k^{-1}(\eta^2), r_k]$. Consequently, the functions κ_i, $i = 1, 2$ in (3.15) are bounded, and (3.1) with $V_{\text{eff}} = V_k$ is Ulam stable on this interval. Moreover, $f_0(r) = A\sqrt{\eta r}\, I_{l+1/2}(\eta r)$ is bounded here, and for low energies $\eta \to 0$ there exists a constant L_2 such that (3.12) holds:

  $$\left|f_0''(r) + \left(\varepsilon^{-2}\lambda_1(r) - \frac{l(l+1)}{r^2} - \eta^2\right) f_0(r)\right| = \left|\varepsilon^{-2}\lambda_1(r) f_0(r)\right| \le L_2(\eta r)^{l+1}\,.$$

  Therefore, there exists a constant L_3 on $(V_k^{-1}(\eta^2), r_k]$ such that

  $$\left|f(r) - f_0(r)\right| \le L_3\,(\eta r)^{l+1}\,.$$

Combining the two steps and setting $C_k := max\{L_1, L_3\}$ completes the proof. □

Note that, in view of the asymptotic behavior of $-\lambda_1(r)$ at $r = 0$ displayed in (2.14), it may be possible to improve the exponent $l + 1$ in (3.19). Moreover, the second step of the proof of Lemma 3.6 can still be carried out under weaker regularity assumptions on $-\lambda_1(r)$.

Finally, we are ready to prove Theorem 1.1.

Proof of Theorem 1.1.
Let us denote E_n^{eff} (resp. E_n^0) as the n-th eigenvalue of the problem (3.1) with the effective potential $-\lambda_1(r)$ in (2.13) (resp. V_0 in (3.3)). By min-max principle (see *e.g.*, [42]), $\lim_{n\to\infty} \left|E_n^{\text{eff}} - E_n^0\right| \to 0$. Here, with the abuse of the notation, we absorbed this error into the systemic error ζ_n in (3.8). By summing up the results of Lemma 3.1, Lemma 3.2, Proposition 3.3 and finally, Lemma 3.6, we obtain (1.13). □

Remark 3.7. In light of the proofs of Proposition 3.3 and Lemma 3.6, the asymptotic behavior of $\lambda_1(r)$ at the origin is crucial for establishing the Efimov effect with eigenvalues of the form (1.13). In fact, for $\Lambda < 0$, the eigenvalue formula (3.8) resembles the expression (1.4) that Vitaly Efimov derived

in [17]. This corresponds to imposing a momentum cutoff on the potential, namely, a nonzero constant short-range core with an inverse-squared tail glued to it.
One might expect that if the constant Λ in (3.6) is replaced by a regular function $\Lambda(r)$ with nonzero value at $r = 0$, then an argument similar to Lemma 3.6 would still yield (3.8). For instance, this is the situation considered by Fonseca *et al.* in [25, 26], where Yamaguchi-type potentials are used. However, this expectation is incorrect.
Repeating the proof of Lemma 3.6 in this setting shows that the right-hand side of (3.16) is replaced by a term of order $(\sqrt{\varepsilon^{-2}\Lambda}\, r_0)^{\frac{1}{2}}$ (see (B.5)). Consequently, in the low-energy limit $\eta \to 0$, this error does not vanish. This means that the dependence of the binding energy on the short-range part of the potential differs from (3.8) with $\Lambda < 0$, because the corresponding matching condition is not satisfied in this case.

Notably, many authors separate short-range and long-range regimes to handle the short-distance behavior, but this typically makes the Efimov spectrum depend on an additional, often unknown parameter. By contrast, we show that the regularity of $-\lambda_1(r)$ together with $-\lambda_1(0) = 0$ already ensures that the Efimov binding energies have the form (1.13). Moreover, the short/long-range split introduces an extra challenge: one must verify that a bound state controlled by the inverse-squared long-range tail is also an eigenvalue for the full potential including the short-range core. This step is typically sidestepped in the literature. As discussed above, even writing a binding-energy formula such as (3.8) with $\Lambda < 0$ and hence, proving the geometrical law (1.2) is delicate unless the short-range part is kept strictly constant.
We conclude this subsection with a brief discussion of possible non-Efimov eigenvalues of the Hamiltonian (3.1). Loosely speaking, a non-Efimov eigenvalue (see, *e.g.*, [38, 33, 24]) is an eigenvalue generated by the short-range part of the interaction and its spatial size is significantly smaller than that of Efimov states. Such eigenvalues do not obey the scaling law (1.2). Consequently, if no non-Efimov eigenvalue is present, the ground state of the system is the first Efimov eigenvalue.

Let $r_0 = \sqrt{2}\frac{3\pi}{4}$ and set $\Lambda = -\lambda_1(r_{\min})$ in (3.6), where $-\lambda_1(r_{\min})$ is the minimum of $-\lambda_1(r)$. Denote by $\jmath_{l+1/2,1}$ the first positive zero of the Bessel function $J_{l+1/2}$ (see [1, section 9.5]). In Proposition 3.8 below we give a sufficient condition ensuring that the ground state of (3.1) coincides with E_1^{eff} in (1.13).
Proposition 3.8. *For a fixed angular momentum $l \geq 0$, the ground state of the Hamiltonian* (3.1) *is the first Efimov eigenvalue, if the mass ratio $\frac{M}{m}$ satisfies:*

$$\frac{M}{m} < \left(\frac{1}{\lambda_1(r_{\min})}\frac{2}{3\pi}\jmath_{l+1/2,1}\right)^2 - \frac{1}{8}\,. \tag{3.20}$$

Proof. Let $u_c^l(r)$ denote the solution of (3.1) with the potential (3.6) and $\Lambda = -\lambda_1(r_{\min})$. Then, from (B.7), using standard Bessel identities (see [1, section 9]) and the scaling (3.7),

$$u_c^l(r) = A\left(\sqrt{\varepsilon^{-2}\,\lambda_1(r_{\min}) - \eta^2}\, r\right)^{1/2} J_{l+1/2}\left(\sqrt{\varepsilon^{-2}\,\lambda_1(r_{\min}) - \eta^2}\, r\right), \qquad r < r_0\,. \tag{3.21}$$

Because $|\lambda_1(r)| \leq |\lambda_1(r_{\min})|$, the Sturm–Picone comparison theorem [14] on $[0, r_0]$ implies that the number of zeros of u_c^l is greater than that of u in (B.7). Hence, for $l \geq 0$, if the first zero of $u_c^l(r)$ (besides $u_c(0) = 0$), occurring at r_c, lies outside $[0, r_0]$, there is no eigenvalue on this interval. Equivalently,

$$\sqrt{\varepsilon^{-2}\,\lambda_1(r_{\min}) - \eta^2}\, r_c \leq j_{l+1/2,1}\,. \tag{3.22}$$

Setting $\eta = 0$ and $r_c = \sqrt{2}\frac{3\pi}{4}$ yields (3.20). $\square$

To illustrate (3.20), for $l = 0$ (resp. $l = 1$) the condition becomes $\frac{M}{m} < 11.24$ (resp. $\frac{M}{m} < 23.12$), to two-digit accuracy, ensuring that no non-Efimov eigenvalue exists.

3.2 Finite scattering length

In this part we study the eigenvalue problem (1.11) with $V_{\text{eff}} = -\lambda_\theta$ for $t_\theta < 1$. We recall that the essential spectrum of $\mathcal{H}_{\text{eff}}$ is $\sigma_{\text{ess}} = [-\frac{(1-t_\theta)^2}{2}, \infty)$. Motivated by (2.15), we introduce the shifted potential

$$V_{\text{sh}}(r, t_\theta) := -\lambda_\theta(r) + \frac{(1-t_\theta)^2}{2}, \qquad t_\theta < 1\,. \tag{3.23}$$

This shifts the entire spectrum by the constant $-\frac{(1-t_\theta)^2}{2}$. In Fig. 2 we depict V_{sh} for $t_\theta = 1$, 0.9, 0.5, 0. Thus, we focus on (3.1) with $V_{\text{eff}} = V_{\text{sh}}$ as in (3.23). We immediately observe that, as $a_\theta(0)$ decreases for $t_\theta < 1$, the short-range well deepens; consequently, for sufficiently small $a_\theta(0)$ the system develops a ground state localized near the origin.

As noted in the introduction, Efimov [17] claimed that the number of bound states is proportional to $\ln \frac{a}{r_0}$, where r_0 is the range of the two-body potential. Fonseca *et al.* [25] investigated this using semiclassical estimates such as Bargmann's bound (see [42] and (3.27) below).

Moreover, when the scattering length is large and the system is close to the unitary limit, the point spectrum of (3.1) is expected to consist of low-energy eigenvalues with large spatial size in configuration space. Note that the spatial structure of such long-range, low-energy bound states differs from molecular bound states. Intuitively, for Efimov states the third particle moves back and forth between the other two, and the size grows logarithmically as $E_n \to 0$ (see [36, Sec. 4.5.2] and references therein).

Let $\mathcal{S}$ denotes the size of the weakest Efimov-like[4] eigenvalue. In the Efimov physics literature it is often suggested that $\mathcal{S} = a$, where a is the two-body scattering length in (1.1) (see, *e.g.*, [17, 25, 36]). In our framework this would correspond to $a_\theta(0)$ (see Remark 2.4). The idea behind the suggestion $\mathcal{S} = a$ is that a generic radial potential in $\mathbb{R}^3$ with scattering length a acts like a hard-sphere of radius a.

This picture can be illustrated in the Born–Oppenheimer setting, where the light-particle Hamiltonian (1.10) is modeled by local point interactions. Assuming $\mathcal{S} = a$ would then mean that the effective

[4] See Remark 3.11.

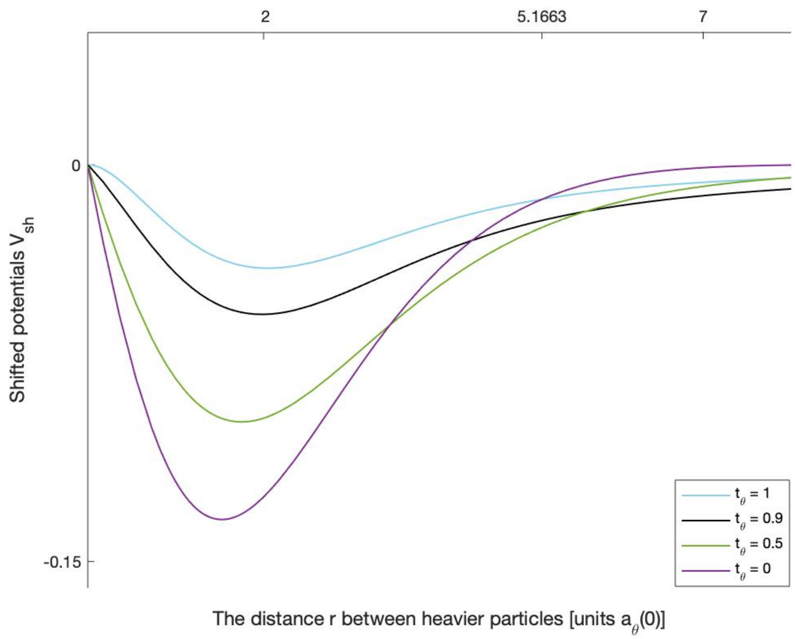

Figure 2: Effective potentials shifted by the constant $\frac{(1-t_\theta)^2}{2}$. The light blue line represents the potential with infinite scattering length $a_\theta(0)$. Decreasing $a_\theta(0)$ increases the depth of the short-range well.

Hamiltonian (3.1) supports low-energy states localized within a sphere of radius at most a, provided a is large.

However, taking $\mathcal{S} = a$ is incompatible with quantitative computations (see Corollary 3.9 and Remark 3.10 below). The main results of this subsection is finding a refined estimate of $\mathcal{S}$ consistent with explicit calculations. Moreover, we trace out Efimov spectrum away from the unitary limit and improve the Bargmann's bound for the number of bound states.
Recall that

$$-\lambda_\theta(r) = -\frac{1}{r^2}\left[W\left(\mathrm{e}^{-\frac{r}{\sqrt{2}}(1-t_\theta)+g_\theta(r)}\right) - \left(-\tfrac{r}{\sqrt{2}}(1-t_\theta) + g_\theta(r)\right)\right]^2, \quad t_\theta \leq 1\,.$$

Our primary interest is the regime close to the unitary limit. Accordingly, for the rest of this subsection we assume $0 \leq t_\theta < 1$, so that $a_\theta(0) \in [\sqrt{2}, \infty)$. Using (2.15) and arguing as in Lemma 3.1, we remove the exponentially decaying oscillation g_θ from $-\lambda_\theta$ for r larger than the scattering length $a_\theta(0)$ and define

$$V_\theta(r) = \begin{cases} -\lambda_\theta(r) + \frac{(1-t_\theta)^2}{2} & \text{if} \quad 0 \leq r \leq a_\theta(0) \\ -\frac{1}{r^2}\left[W\left(\mathrm{e}^{-\frac{r}{\sqrt{2}}(1-t_\theta)}\right) + \frac{r}{\sqrt{2}}(1-t_\theta)\right]^2 + \frac{(1-t_\theta)^2}{2} & \text{if} \quad r > a_\theta(0) \end{cases}, \quad 0 \leq t_\theta < 1\,. \tag{3.24}$$

Moreover, we obtain the following estimate for $r > a_\theta(0)$ by the Lemma 2.3

$$V_\theta\big(r\big|_{r>a_\theta(0)}\big) = -\left(\frac{\mathrm{e}^{-2r/a_\theta(0)}}{r^2} + \frac{2}{a_\theta(0)}\frac{\mathrm{e}^{-r/a_\theta(0)} - \mathrm{e}^{-2r/a_\theta(0)}}{r}\right) + O\left(\frac{\mathrm{e}^{-3r/\sqrt{2}}}{r}\right). \tag{3.25}$$

Apart from the term $\frac{2}{a_\theta(0)}\frac{\mathrm{e}^{-2r/a_\theta(0)}}{r}$, the estimate (3.25) also appeared in [17, Eq. (27)] and [25, Eq. (45)]. Moreover, in the region that the potential V_θ in (3.24) is below $-\lambda_1(r)$ with inverse-squared behavior, the min–max principle implies that the number of eigenvalues of (1.11) with $V_{\text{eff}} = V_\theta$ is greater than or equal to that with $V_{\text{eff}} = -\lambda_1(r)$. Hence, the radius at which these two potentials intersect provides a suitable estimate for $\mathcal{S}$.

Corollary 3.9. *For fixed $0 \le t_\theta < 1$, the parameter $\mathcal{S}$ is given by the first root (other than $r = 0$) of $V_\theta(r) + \lambda_1(r) = 0$. In particular, using (3.25) and (2.15), one can estimate $\mathcal{S}$ from*

$$-\left(\frac{\mathrm{e}^{-2\mathcal{S}/a_\theta(0)}}{\mathcal{S}^2} + \frac{2}{a_\theta(0)}\frac{\mathrm{e}^{-\mathcal{S}/a_\theta(0)} - \mathrm{e}^{-2\mathcal{S}/a_\theta(0)}}{\mathcal{S}}\right) + O\left(\mathrm{e}^{-3\mathcal{S}/\sqrt{2}}\right) = -\frac{W^2(1)}{\mathcal{S}^2}. \tag{3.26}$$

Therefore, $\mathcal{S} \simeq 2.80\, a_\theta(0)$ to two digits.

Remark 3.10. As discussed earlier, the estimate $\mathcal{S} \simeq 2.80\, a_\theta(0)$ cannot be reconciled with the intuition from local point interactions, even though (3.25) is reported in [17, 25]. In fact, the long-range behavior of $-\lambda_\theta$ matches its local analogue (2.17) if one sets $\alpha = \frac{t_\theta - 1}{4\sqrt{2}\pi}$ (see Remark 2.4); thus, Corollary 3.9 follows readily. However, this is not the only issue with the local intuition.
Efimov [17] and later Fonseca *et al.* [25] describe the effective potential in (1.11) away from unitary limit as having three ranges: a short-range part (irrelevant for $\mathcal{S}$), an intermediate range with the same inverse-squared behavior as at unitary limit, and a long-range Yukawa tail. The intermediate range, of length a, is said to support the first m Efimov energies E_i (the initial part of the sequence E_n^{eff} in (1.13)), while the remainder fades into the Yukawa tail. Taken literally, this picture would make the potential discontinuous at $r = a$, in conflict with (3.25); hence it is not physically consistent.
Furthermore, for any angular momentum $l \ge 0$, Fonseca *et al.* [25] applied Bargmann's bound (3.27) to (3.1) with (3.24) and obtain an upper bound $n_l(V_\theta)$ on the number of eigenvalues. One readily finds $n_l(V_\theta) \simeq 0.53\,\varepsilon^{-2}/(2l+1)$ over the range $a_\theta(0) < r < \mathcal{S}$, independent of $a_\theta(0)$ (or $4\pi\alpha$ in the local model, see (3.28) below). This is rather large for the mass-imbalanced system of two heavy and one light particle. For example, with the angular momentum $l = 1$, if one substitutes the critical mass ratio $\mathcal{M}_1^*$ in (3.5) in $0.53\,\varepsilon^{-2}/(2l+1)$, they obtain $n_l(V_\theta) > 1.16$ on the interval $(a_\theta(0), \mathcal{S})$, which is incompatible with the description in [25].

Due to the low-energy nature of Efimov physics, Bargmann's bound (see [42, Theorem XIII.9]) gives a nearly sharp upper bound on the number of negative eigenvalues of (3.1) with $V_{\text{eff}} = V_\theta$ in (3.24). For fixed $l \ge 0$, denote by $n_l(V_\theta)$ the number of negative binding energies. Bargmann's bound is then given by the right-hand side (RHS) of (3.27):

$$n_l(V_\theta) \le \frac{\varepsilon^{-2}}{(2l+1)} \int_0^\infty r\,|V_\theta(r, t_\theta)|\,\mathrm{d}r. \tag{3.27}$$

To evaluate the RHS of (3.27), we split the positive half-line into three intervals: $[0, a_\theta(0)]$, $(a_\theta(0), \mathcal{S}]$, and $(\mathcal{S}, +\infty)$. On $[0, a_\theta(0)]$ we use numerics. For example, for $t_\theta = 0.9$ with $a_\theta(0) = 10\sqrt{2}$,

$$\int_0^{10\sqrt{2}} r\,|V_\theta(r, 0.9)|\,\mathrm{d}r = 1.1042,$$

as computed in MATLAB to four-decimal accuracy.

For $r > a_\theta(0)$ we use the estimate (3.25). Set $\zeta := r/a_\theta(0)$; then, on $(a_\theta(0), \mathcal{S}]$,

$$\begin{aligned}
&\frac{\varepsilon^{-2}}{(2l+1)} \int_{a_\theta(0)}^{\mathcal{S}} \frac{\mathrm{e}^{-2r/a_\theta(0)}}{r} + \frac{2}{a_\theta(0)} \left(\mathrm{e}^{-r/a_\theta(0)} - \mathrm{e}^{-2r/a_\theta(0)}\right) \mathrm{d}r \\
&= \frac{\varepsilon^{-2}}{(2l+1)} \left(\int_1^{\mathcal{S}} 2\left(\mathrm{e}^{-\zeta} - \mathrm{e}^{-2\zeta}\right) + \frac{\mathrm{e}^{-2\zeta}}{\zeta} \mathrm{d}\zeta \right) \\
&= \frac{\varepsilon^{-2}}{(2l+1)} \left(2\mathrm{e}^{-x} - \mathrm{e}^{-2x} - \Gamma(0, 2x)\right)\Big|_{x=1}^{x=2.8} \simeq 0.5308\,\frac{\varepsilon^{-2}}{(2l+1)}\,,
\end{aligned} \tag{3.28}$$

where we used $\mathcal{S} = 2.8\,a_\theta(0)$ from Corollary 3.9 and Γ is the incomplete gamma function (see [1, §6.5]). Similarly, on the interval $(\mathcal{S}, +\infty)$,

$$\frac{\varepsilon^{-2}}{(2l+1)} \int_{\mathcal{S}}^{\infty} \frac{\mathrm{e}^{-2r/a_\theta(0)}}{r} + \frac{2}{a_\theta(0)} \left(\mathrm{e}^{-r/a_\theta(0)} - \mathrm{e}^{-2r/a_\theta(0)}\right) \mathrm{d}r \simeq 0.1184\,\frac{\varepsilon^{-2}}{(2l+1)}\,. \tag{3.29}$$

From (3.28), the logarithmic dependence of Bargmann's bound on $a_\theta(0)$ is apparent. Indeed, fixing $r = r_0$ and setting $\zeta_0 := r_0/a_\theta(0)$, as $a_\theta(0) \to \infty$ we have $\zeta_0 \to 0$, and the incomplete gamma function satisfies

$$-\Gamma(0, 2\zeta_0) = \ln(2\zeta_0) + \gamma - 2\zeta_0 + O\big(\zeta_0^2\big)\,,$$

where γ is Euler's constant.

Finally, the idea of proportionality of the number of eigenvalues to $-\ln(a/r_0)$ comes from using (2.17) with a finite-range cutoff r_0. Replacing that by the shifted potentials (3.23) corrects the $\ln r_0$ term and, in turn, yields a substantially sharper Bargmann bound.

We conclude this section with a remark on the energy eigenvalues of (3.1) with $V_{\text{eff}} = V_{\text{sh}}$ from (3.23).

Remark 3.11. As discussed above, for $t_\theta < 1$ the potential $-\lambda_\theta(r)$ does not exhibit an inverse-squared tail. Hence, interpreting the eigenvalues that localize within the sphere of radius $\mathcal{S}$ as genuine Efimov states obeying the geometric law (1.2) is not accurate. In this regime, the shifted effective potential $V_{\text{sh}}(r)$ lies below $-\lambda_1(r)$ for all r. Consequently, the wave function associated with any eigenvalue of (1.11) in this case is no longer given by (3.10), *i.e.*,

$$D\,\frac{K_{i\beta}(\sqrt{\varepsilon^{-2}\,|E_n|})}{\sqrt{r}}\,.$$

Moreover, the discrepancy grows as t_θ departs from the unitary limit $t_\theta = 1$; for sufficiently large mass ratio, this mismatch can even yield additional eigenvalue(s). For these reasons, we use the term *Efimov-like* eigenvalues to distinguish them from the Efimov spectrum (1.13) that satisfies (1.2).

4 Conclusions

In this work, we studied a $2+1$ mass-imbalanced particle system in the Born–Oppenheimer approximation, where the heavy–light interactions were modeled by zero-range (delta-type) potentials.
Using von Neumann's extension theory, we introduced a class of point interactions in the Hamiltonian of the light particle which, unlike standard local point interactions, remain regular as the distance between the heavy centers tends to zero. We showed that this construction is consistent with the expected physical behavior of a $2+1$ system. Moreover, we proved the Efimov effect for arbitrary angular momentum, where the Efimov eigenvalues depend solely on the mass ratio of the particles and the angular momentum. Consequently, the so-called three-body parameter, usually introduced to encode short-range details, is absent here, as expected for a zero-range model. We also derived a sufficient condition ensuring that the ground state of the system corresponds to the first Efimov eigenvalue.
In addition, we traced the Efimov spectrum away from the unitary limit and discussed how qualitative interpretations based on local point interactions lead to inconsistencies with the quantitative features of the three-body system. We showed that the size of the weakest bound state near the threshold is roughly three times larger than the two-body scattering length, contrary to the common assumption that the two scales coincide. Finally, we refined Bargmann's bound on the number of bound states and analyzed how the spectrum away from the unitary limit differs from the Efimov spectrum in the unitary regime.
The validity of the Born–Oppenheimer picture is often taken for granted in the Efimov physics literature. A natural next step is to quantify the error of this approximation rigorously. We briefly recall the standard procedure from molecular physics.
Let E_1^ε denote the isolated ground-state energy of the three-body Hamiltonian (1.9). The goal is to show that $E_1^{\mathrm{eff}} \to E_1^\varepsilon$ as $\varepsilon^2 \to 0$, where E_1^{eff} is the ground state of the effective Hamiltonian $\mathcal{H}_{\mathrm{eff}}$. To this end, it is common (see, *e.g.*, [31, 29]) to introduce the direct integral on the Hamiltonian of the light particle (or its quadratic form)

$$\mathcal{H}_{x,R} := \int_{\mathbb{R}}^{\oplus} \mathcal{H}_x(R)\,\mathrm{d}R\,,$$

and (formally) rewrite (1.9) as

$$\mathcal{H}_\varepsilon^{b/f} = -\varepsilon^2 \mathit{\Delta}_R + \mathcal{H}_{x,R}\,.$$

In this setting, $\mathit{\Psi}(x,R) = \psi(x,R)\mathit{\Phi}(R)$ is proportional to the eigenfunction of the three-body Hamiltonian $\mathcal{H}_\varepsilon^{b/f}$.
Applying this approach in Efimov physics is, however, delicate. In molecular physics the mass ratio typically ranges from about 1.8×10^3 to 3.7×10^5, so it is natural to regard ε as a small parameter. In contrast, in most systems suitable to observe the Efimov effect in practice, the mass ratio is comparatively small (see, e.g., [50, 39] for the ^{6}Li–^{133}Cs case). Moreover, in the limit $\varepsilon^2 \to 0$, all eigenvalues in the Efimov spectrum (1.13) converge to zero, independently of n, and conditions such as

(3.5) or (3.20) become irrelevant.
Furthermore, unlike the case of smooth potentials V in (1.9), for zero-range interactions the product $\Psi(x,R) = \psi(x,R)\Phi(R)$ does not, in general, belong to the domain of $\mathcal{H}_\varepsilon^{b/f}$ because it fails to satisfy the required boundary conditions in R (see [10] for a one-dimensional discussion). Finally, zero is an accumulation point of the Efimov spectrum; hence there is no spectral gap at the threshold.
To address this issue with the domain, it is possible to adapt the general framework of [31] at the level of the quadratic forms associated with the operators, although this remains challenging due to the lack of a spectral gap near zero.
To summarize, the validity of Born-Oppenheimer approximation in Efimov physics is far from understood. Nevertheless, this formal framework captures the qualitative features of the Efimov effect and provides a better understanding of the three-body problem, whose spectral analysis is considerably harder and more involved.

Acknowledgements

I am especially grateful to Rodolfo Figari for his guidance and many helpful discussions that contributed to the development of this work. I also thank Andrea Posilicano, Claudio Cacciapuoti, and Alessandro Teta for constructive conversations that supported various parts of this work.
The Author also acknowledge funding from the Next Generation EU-Prin project 2022CHELC7 "Singular Interactions and Effective Models in Mathematical Physics" and the support of the National Group of Mathematical Physics (GNFM-INdAM).

Appendix A Proof of Lemma 2.3

Define

$$\omega(r,t_\theta) := -\tfrac{r}{\sqrt{2}}\,(1-t_\theta) + g_\theta(r), \qquad r \geq 0\,. \tag{A.1}$$

It is evident that $u = f^{-1}(\omega) = W(\mathrm{e}^{\omega}) - \omega$ is the inverse function of $\omega = f(u) = \mathrm{e}^{-u} - u$. The main tool here is the Lagrange inversion theorem (see [1, section 3.6]), *i.e.*, f^{-1} is analytic at $\omega_0 = f(u_0)$, if $f'(u_0) \neq 0$, provided f is analytic itself.
Clearly, $\omega(r,t_\theta)$ in (A.1) is a composition of analytic functions, so it is analytic itself. To satisfy the conditions of Lagrange inversion theorem, $\omega_0 = f(u_0)$ must belong to a domain $\mathcal{V}$ that

$$f'(u_0) \neq 0, \quad f(u_0) \in \mathcal{V}\,.$$

Since $f'(u) = -(\mathrm{e}^{-u}+1)$, the critical points $u_c = -\,i(2k+1)\pi$, $k \in \mathbb{Z}$ satisfy $f'(u) = 0$. The corresponding critical values under the map f are

$$\omega_c = f(u_c) = -1 + i(2k+1)\pi, \qquad k \in \mathbb{Z}.$$

The ones closest to the real axis are $\omega_c^{\pm} = -1 \pm i\pi$. By Lagrange inversion, the Taylor series of f^{-1} about ω_0 converges in the open disk centered at ω_0 with radius equal to the distance from ω_0 to the set of critical values:

$$\kappa := \operatorname{dist}\big(\omega_0, \{\omega_c\}_{k\in\mathbb{Z}}\big) = \inf_{k\in\mathbb{Z}} \big\|\omega_0 - (-1 + i(2k+1)\pi)\big\|.$$

In particular, if $\omega_0 \in \mathbb{R}$ in this case, then the nearest critical values are $\omega_c^{\pm}$, so $\kappa = \|\omega_0 - \omega_c^{\pm}\|$.

For $\omega_0 = \omega(r, t_\theta)$ from (A.1) with $t_\theta \leq 1$ and $r \geq 0$, we have $\kappa > 0$, so the series for f^{-1} is valid. Moreover, the factor r^{-2} has a removable singularity at $r = 0$; hence $-\lambda_\theta(r)$ extends analytically to the real half-line, and the asymptotics (2.14)–(2.15) follow.

At $r = 0$ we have $\omega(0, t_\theta) = 1$. Hence, $\kappa = \sqrt{\pi^2+4}$ and the Taylor series of f^{-1} about $\omega_0 = 1$ has radius $\kappa = \sqrt{\pi^2+4}$. However, the distance that we can vary r while keeping $\omega(r, t_\theta)$ inside the disk $\mathbb{D}(1, \kappa)$ depends on t_θ. Set

$$u(r) := f^{-1}(\omega(r, t_\theta))\,,$$

there exists $\delta(t_\theta)$ the range that $|\omega(r, t_\theta) - 1| < \kappa$ for $0 \leq r < \delta(t_\theta)$. We readily see the admissible r-range shrinks as $t_\theta \to -\infty$, so $\delta(t_\theta) \to 0$. Moreover, at the unit value $t_\theta = 1$ we have $-\sqrt{2}\,\mathrm{e}^{-5\pi/4} \leq \omega(r, 1) \leq 1$, so $\omega(r, 1) \in \mathbb{D}(1, \kappa)$ for all $r \geq 0$. Therefore, the admissible r-range is unbounded radius to the right in the r-variable).

Next, we now show that, for $t_\theta < 1$, the Taylor series in r of $u(r)$ about $r = a_\theta(0)$ converges for all $r \geq a_\theta(0)$ *i.e.*, it is unbounded in the variable r as well. Recall $a_\theta(0) = \frac{\sqrt{2}}{1-t_\theta}$ and, at $r = a_\theta(0)$,

$$\omega_0 := \omega\big(a_\theta(0), t_\theta\big) = -1 + g_\theta\big(a_\theta(0)\big).$$

With the same reasoning as before, the Taylor series of f^{-1} is convergent about ω_0 with the radius π. Therefore, if $|\omega(r, t_\theta)| \leq \pi$, Taylor series of $u(r)$ about $r = a_\theta(0)$ converges for every $r \geq a_\theta(0)$. Additionally, if $\omega(r, t_\theta) \leq -1$, the Taylor series of the term $W(\mathrm{e}^{\omega})$ is convergent for any r and again, the radius of convergence of Taylor series of $u(r)$ about the point $a_\theta(0)$ is infinite to the right. Summing up these two conditions, we need to show $\omega(r, t_\theta) \leq \pi$ for $r > a_\theta(0)$. We verify it in two ranges of t_θ.

1) If $-1 < t_\theta < 1$, then $g_\theta(r) < \sqrt{2}$ and $-\frac{r}{\sqrt{2}}(1 - t_\theta) \leq -1$ for all $r \geq a_\theta(0)$. Hence the condition $\omega(r, t_\theta) \leq \pi$ is satisfied.

2) If $t_\theta < -1$, we have trivial inequalities

$$-\frac{r}{\sqrt{2}} + e^{-r/\sqrt{2}} \cos\frac{r}{\sqrt{2}} \leq 1, \qquad \frac{r}{\sqrt{2}} + e^{-r/\sqrt{2}} \sin\frac{r}{\sqrt{2}} \geq 0\,.$$

Therefore, $\omega(r, t_\theta) \leq 1$, $t_\theta < -1$. Consequently, for every $t_\theta < 1$ the map $r \mapsto u(r) = f^{-1}(\omega(r, t_\theta))$ is analytic on the entire half-line $[a_\theta(0), \infty)$, and its Taylor series at $r = a_\theta(0)$ converges for all $r \geq a_\theta(0)$.

Appendix B Proof of Proposition 3.3

By considering (3.7), we can rewrite the eigenvalue problem (3.1) as

$$u'' - \left(\frac{l(l+1)}{r^2} + \eta^2 + \varepsilon^{-2}\Lambda \right) u = 0 \qquad \text{for } r < r_0 \tag{B.1}$$

$$u'' + \left(\frac{\beta^2 + 1/4}{r^2} - \eta^2 \right) u = 0 \qquad \text{for } r > r_0 \tag{B.2}$$

with the boundary conditions

$$u \in L^2(\mathbb{R}^+), \qquad u(0) = 0, \qquad \lim_{r \to 0} r^{-(l+1)} u(r) = 1 \,. \tag{B.3}$$

These equations are respectively modified Bessel equations of real order $l + 1/2$ and imaginary order $\nu = i\beta$. As a result, the general solution of (B.1) is a linear combination of modified Bessel functions of the first and second kind. However, the modified Bessel function of the first kind I with purely imaginary order becomes complex on the positive real axis, so it not admissible as the solution of (B.2) that satisfies (B.3). Therefore, Dunster [15] introduces the modified Bessel function L_γ:

$$L_\gamma(z) = \frac{\pi i}{2\sin(\gamma\pi)} \left\{ I_\gamma(z) + I_{-\gamma}(z) \right\} \quad (\gamma \neq 0) \tag{B.4}$$

As a result, the general solution for (B.2) can be written as a linear combination of the Bessel functions $L_{i\beta}(\eta r)$ and $K_{i\beta}(\eta r)$. Therefore, we have the following form of the solutions:

$$u(r < r_0) = A \,(\sqrt{\eta^2 + \varepsilon^{-2}\Lambda}\, r)^{\frac{1}{2}} I_{l+1/2}(\sqrt{\eta^2 + \varepsilon^{-2}\Lambda}\, r) + B \,(\sqrt{\eta^2 + \varepsilon^{-2}\Lambda}\, r)^{\frac{1}{2}} K_{l+1/2}(\sqrt{\eta^2 + \varepsilon^{-2}\Lambda}\, r), \tag{B.5}$$

$$u(r > r_0) = C\, \sqrt{r} L_{i\beta}(\eta\, r) + D\, \sqrt{r} K_{i\beta}(\eta\, r), \tag{B.6}$$

where A, B, C, D are arbitrary complex constants. Note that, the modified Bessel function $L_{i\beta}$ grows exponentially fast at infinity and the modified Bessel function $K_{l+1/2}$ is singular at the origin. Taking into account this property alongside the boundary conditions (B.3), we obtain $B = C = 0$ in (B.5) and (B.6). Thus,

$$u(r) = \begin{cases} A \,(\sqrt{\eta^2 + \varepsilon^{-2}\Lambda}\, r)^{\frac{1}{2}} I_{l+1/2}(\sqrt{\eta^2 + \varepsilon^{-2}\Lambda}\, r)\,, & r < r_0 \\ D\, \sqrt{r} K_{i\beta}(\eta r)\,, & r > r_0 \end{cases} . \tag{B.7}$$

Let us denote $\tau_0 = \eta r_0$ and recall $\xi = (\sqrt{\eta^2 + \varepsilon^{-2}\Lambda}\, r_0)$. The solution has to satisfy matching conditions, *i.e.* the continuity of the function and its derivative in $r = r_0$. This condition implies that the coefficient A, D have to satisfy:

$$\begin{cases} \sqrt{\xi} I_{l+1/2}(\xi)\, A \; - \; \sqrt{r_0} K_{i\beta}(\tau_0)\, D & = 0 \\ \left(\frac{\sqrt{\xi}}{2r} I_{l+1/2}(\xi) + \frac{\sqrt{\xi}\xi}{r} I'_{l+1/2}(\xi) \right) A \; - \; \left(\frac{1}{2\sqrt{r_0}} K_{i\beta}(\tau_0) + \eta \sqrt{r_0} K'_{i\beta}(\tau_0) \right) D & = 0 \end{cases} \tag{B.8}$$

This linear homogeneous system has non-zero solutions if and only if its determinant is equal to zero. In other words, we have to satisfy:

$$K_{i\beta}(\tau_0) = 2\tau_0 f(\xi)\, K'_{i\beta}(\tau_0) \qquad \text{with} \qquad f(\xi) := \frac{I_{l+1/2}(\xi)}{2\xi\, I'_{l+1/2}(\xi)} = \frac{I_{l+1/2}(\xi)}{\xi\left(I_{l-1/2}(\xi) + I_{l+3/2}(\xi)\right)}\,. \tag{B.9}$$

Note that by the asymptotic behaviors of the functions $I_{l\pm 1/2}$ (see [1, section 9.6]) we have:

$$\lim_{\xi\to 0} f(\xi) = \frac{1}{2l+1}\,.$$

Furthermore, for $\tau_0 \to 0$ we also have (see [15]):

$$K_{i\beta}(\tau_0) = C_\beta \sin\Big(\beta \ln\frac{\tau_0}{2} - \phi_\beta\Big) + O(\tau_0^2)\,, \qquad K'_{i\beta}(\tau_0) = C_\beta \frac{\beta}{\tau_0} \cos\Big(\beta \ln\frac{\tau_0}{2} - \phi_\beta\Big) + O(\tau_0) \tag{B.10}$$

where

$$C_\beta = -\sqrt{\frac{\pi}{\beta\sinh(\beta\pi)}} \quad \text{and} \quad \phi_\beta = \arg\Gamma(1+i\beta)\,. \tag{B.11}$$

As a result, the equation (B.9) in the limit $\tau_0 \to 0$ can be rewritten as:

$$\sin\Big(\beta \ln\frac{\tau_0}{2} - \phi_\beta\Big) - 2\beta f(\xi) \cos\Big(\beta \ln\frac{\tau_0}{2} - \phi_\beta\Big) = F(\tau_0) \tag{B.12}$$

where F is (at least) continuous and $F(\tau_0) = O(\tau_0^2)$ for $\tau_0 \to 0$. With the change of coordinates $\theta = \beta \ln\frac{\tau_0}{2} - \phi_\beta$ and the equation, we have (B.12):

$$\theta = \arctan\left(2\beta\, f(\xi) + \frac{F\left(\tau_0\right)}{cos\theta}\right) \tag{B.13}$$

Note that $\frac{F(\tau_0)}{\cos\theta}$ with $\tau_0 = 2\,\mathrm{e}^{\frac{\phi_\beta}{\beta}}\,\mathrm{e}^{\frac{\theta}{\beta}}$ tends to zero with the order of $O\left(\tau_0^2\right)$ as $\tau_0 \to 0$. Also, $f(\xi)$, $\xi \in \mathbb{C}$ is analytic in the unit disk in vicinity of the origin.

As a result, for any value of r_0, there exists an infinite sequence θ_n of solutions of equation (B.13) as $\tau_0 \to 0$, with $\theta_n < 0$ and $\lim\limits_{n\to+\infty} \theta_n = -\infty$.

To conclude the proof, we have to show that the sequence of $-(\eta_n)^2$, corresponds this sequence of θ_n as the solutions of (B.13) can be written in the form (3.8). Let us denote by $-\left(\eta_n^0\right)^2$ as the solutions of (B.13) corresponds to $F(\tau_0) = 0$. We have:

$$-\left(\eta_n^0\right)^2 = \varepsilon^{-2} E_n^0 = -\frac{4}{r_0^2}\,\mathrm{e}^{\frac{2}{\beta}\left(\arctan\left(\frac{2\beta}{2l+1}\right) + \phi_\beta - n\pi\right)} \tag{B.14}$$

It is evident that the function $\eta_n = \frac{2}{r_0}\,\mathrm{e}^{\frac{\phi_\beta}{\beta}}\,e^{\frac{\theta_n}{\beta}}$ is a differentiable function of η (see (B.13)) with bounded derivative which converges to 0 for $\eta_n \to 0$. Consequently,

$$-(\eta_n)^2 = -(\eta_n^0)^2 + \zeta_n\,,$$

where $\zeta_n \to 0$ as $n \to \infty$.

References

[1] M. Abramovitz and I.A. Stegun. *Handbook of Mathematical Functions: with Formulas, Graphs, and Mathematical Tables*. Dover, New York, 1965.

[2] S. Albeverio, S. Fassari, and F. Rinaldi. The behaviour of the three-dimensional Hamiltonian $-\mathit{\Delta}+\lambda[\delta(x+x_0)+\delta(x-x_0)]$ as the distance between the two centres vanishes. *Nanosystems: Physics, Chemistry, Mathematics*, 8(2):153–159, 2017.

[3] S. Albeverio, F. Gesztesy, R. Høegh-Krohn, and H. Holden. *Solvable Models in Quantum Mechanics*. AMS Chelsea Publishing, Providence, RI, 2 edition, 2005. With an appendix by Pavel Exner.

[4] D. R. Anderson, M. Onitsuka, and D. O'Regan. Best Ulam constants for damped linear oscillators with variable coefficients. *Journal of Mathematical Analysis and Applications*, 543(2, Part 1):128908, 2025.

[5] G. Basti, C. Cacciapuoti, D. Finco, and A. Teta. Three-Body Hamiltonian with Regularized Zero-Range Interactions in Dimension Three. *Annales Henri Poincaré*, 24:223–276, 2021.

[6] G. Basti and A. Teta. Efimov effect for a three-particle system with two identical fermions. *Annales Henri Poincaré*, 18(12):3975–4003, 2017.

[7] H. Bethe and R. Peierls. Quantum theory of the diplon. *Proceedings of the Royal Society of London. Series A - Mathematical and Physical Sciences*, 148(A):146–156, 1935.

[8] E. Braaten and H.-W. Hammer. Universality in few-body systems with large scattering length. *Physics Reports*, 428(5):259–390, 2006.

[9] G. Breit. The Scattering of Slow Neutrons by Bound Protons. I. Methods of Calculation. *Phys. Rev.*, 71:215–231, 1947.

[10] C. Cacciapuoti, A. Posilicano, and H. Saberbaghi. The born-oppenheimer approximation for a 1d 2+ 1 particle system with zero-range interactions. *arXiv preprint arXiv:2506.21457*, 2025.

[11] R. M. Corless, G. H. Gonnet, D. E. G. Hare, D. J. Jeffrey, and D. E. Knuth. On the Lambert-W function. *Adv. Comput. Math.*, 5:329–359, 1996.

[12] L. Cădariu, D. Popa, and I. Raşa. Ulam stability of a second linear differential operator with nonconstant coefficients. *Symmetry*, 12(9), 2020.

[13] L. Dabrowski and H. Grosse. On nonlocal point interactions in one, two, and three dimensions. *Journal of Mathematical Physics*, 26:2777–2780, 1985.

[14] J. B. Diaz and J. R. McLaughlin. Sturm comparison theorems for ordinary and partial differential equations. *Bull. Am. Math. Soc.*, 75:335–339, 1969.

[15] T. M. Dunster. Bessel functions of purely imaginary order, with an application to second-order linear differential equations having a large parameter. *SIAM Journal on Mathematical Analysis*, 21(4):995–1018, 1990.

[16] V. Efimov. Energy levels arising from resonant two-body forces in a three-body system. *Physics Letters B*, 33:563–564, 1970.

[17] V. Efimov. Energy levels of three resonantly interacting particles. *Nuclear Physics A*, 210:157–188, 1973.

[18] M. A. Efremov, L. Plimak, B. Berg, M. Yu. Ivanov, and W. P. Schleich. Efimov states in atom-molecule collisions. *Phys. Rev. A*, 80:022714, 2009.

[19] D. Fermi, D. Ferretti, and A. Teta. Rigorous derivation of the Efimov effect in a simple model. *Letters in Mathematical Physics*, 113(6), 2023.

[20] E. Fermi. Sul moto dei neutroni nelle sostanze idrogenate. *Ricerca Scientifica*, 7(2):13–52, 1936.

[21] D. Ferretti and A. Teta. Some remarks on the regularized hamiltonian for three bosons with contact interactions. In *Quantum Mathematics I*, pages 229–246, Singapore, 2023. Springer Nature Singapore.

[22] D. Ferretti and A. Teta. Hamiltonians for quantum systems with contact interactions. *arXiv preprint arXiv:2407.06876*, 2024.

[23] R. Figari, H. Saberbaghi, and A. Teta. On a family of finitely many point interaction hamiltonians free of ultraviolet pathologies. *J. Phys. A: Math. Theor.*, 57(5), 2024.

[24] S. Fisher, O. Ogunnaike, and L. Levitov. Three-body bound states of quantum particles: Higher stability through braiding. *Phys. Rev. A*, 109:043323, 4 2024.

[25] A.C. Fonseca, E.F. Redish, and P.E. Shanley. Efimov effect in an analytically solvable model. *Nuclear Physics A*, 320(2):273–288, 1979.

[26] A.C. Fonseca and P.E. Shanley. Model three-body problem in the molecular mass limit. *Annals of Physics*, 117(2):268–291, 1979.

[27] D. G. Gaidashev. Chapter 2: The cauchy-kovalevskaya theorem. `https://www2.math.uu.se/~danga916/1MA216/CK.pdf`, 2013. Lecture notes, Department of Mathematics, Uppsala University.

[28] M. Gallone and A. Michelangeli. Self-adjoint extension schemes and modern applications to quantum hamiltonians. *Springer Monographs in Mathematics*, 2022.

[29] T. Jecko. On the mathematical treatment of the Born-Oppenheimer approximation. *Journal of Mathematical Physics*, 55(5):053504, 05 2014.

[30] V. F. Kharchenko. Solution of the Skornyov-Ter-Martirosyan equations for three nucleons with cut off at large momenta. *Yadern. Fiz. 16: No. 2, 310-15(Aug 1972).*, 1 1972.

[31] D. Krejčiřík, N. Raymond, J. Royer, and P. Siegl. Reduction of dimension as a consequence of norm-resolvent convergence and applications. *Mathematika*, 64(2):406–429, 2018.

[32] F. Loran and A. Mostafazadeh. Renormalization of multi-delta-function point scatterers in two and three dimensions, the coincidence-limit problem, and its resolution. *Annals of Physics*, 443:168966, 2022.

[33] J. L. Miller. Efimov trimers imaged for the first time. *Physics Today*, 68(7), 7 2015.

[34] R. A. Minlos and L. D. Faddeev. Comment on the problem of three particles with point interactions. *Soviet Phys. JETP*, 14(6):1315–1316, 1962.

[35] R. A. Minlos and L. D. Faddeev. On the point interaction for a three-particle system in quantum mechanics. *Soviet Phys. Dokl.*, 6(12):1072–1074, 1962.

[36] P. Naidon and S. Endo. Efimov Physics: a review. *Rept. Prog. Phys.*, 80(5):056001, 2017.

[37] R. G. Newton. Analytic properties of radial wave functions. *Journal of Mathematical Physics*, 1(4):319–347, 07 1960.

[38] H.-C. Nägerl, T. Kraemer, M. Mark, P. Waldburger, J. G. Danzl, B. Engeser, A. D. Lange, K. Pilch, A. Jaakkola, C. Chin, and R. Grimm. Experimental Evidence for Efimov Quantum States. *AIP Conference Proceedings*, 869(1):269–277, 11 2006.

[39] R. Pires, J. Ulmanis, S. Häfner, M. Repp, A. Arias, E. D. Kuhnle, and M. Weidemüller. Observation of Efimov Resonances in a Mixture with Extreme Mass Imbalance. *Phys. Rev. Lett.*, 112:250404, 2014.

[40] M. C. Reed and B. Simon. *Functional analysis*, volume 1 of *Methods of Modern Mathematical Physics*. Academic Press, New York, 1972.

[41] M. C. Reed and B. Simon. *Methods of Modern Mathematical Physics, Vol. II: Fourier Analysis, Self-Adjointness*, volume 2. Academic Press, New York, 1975. Often referred to as Volume 2.

[42] M. C. Reed and B. Simon. *Analysis of Operators*, volume 4 of *Methods of Modern Mathematical Physics*. Academic Press, New York, 1978.

[43] M. C. Reed and B. Simon. *Scattering theory*, volume 3 of *Methods of Modern Mathematical Physics*. Academic Press, New York, 1979.

[44] D. S. Rosa, T. Frederico, G. Krein, and M. T. Yamashita. Efimov effect in a D-dimensional Born–Oppenheimer approach. *Journal of Physics B: Atomic, Molecular and Optical Physics*, 52(2):025101, 2018.

[45] H. Saberbaghi. On a family of finitely many point interactions Hamiltonians free of ultraviolet pathologies in two and three dimensions. 2025.

[46] M. Schechter. *Operator Methods in Quantum Mechanics.* North Holland, 1981.

[47] A. V. Sobolev. The efimov effect. discrete spectrum asymptotics. *Communications in Mathematical Physics*, 156(1):101–126, 1993.

[48] H. Tamura. The Efimov effect of three-body Schrödinger operators: Asymptotics for the number of negative eigenvalues. *Nagoya Mathematical Journal*, 130:55–83, 1993.

[49] L. H. Thomas. The interaction between a neutron and a proton and the structure of H^3. *Phys. Rev.*, 47:903–909, 1935.

[50] S. Tung, K. Jiménez-García, J. Johansen, C. V. Parker, and C. Chin. Geometric Scaling of Efimov States in a $^6\mathrm{Li} -^{133}\mathrm{Cs}$ Mixture. *Phys. Rev. Lett.*, 113:240402, 2014.

[51] Y. Wang, J. Wang, J. P. D'Incao, and C. H. Greene. Universal three-body parameter in heteronuclear atomic systems. *Phys. Rev. Lett.*, 109:243201, 2012.

[52] D. R. Yafaev. On the theory of the discrete spectrum of the three-particle schrödinger operator. *Mathematics of the USSR-Sbornik*, 23(4):535–559, 1974.

[53] Y. Yamaguchi. Two-Nucleon Problem When the Potential Is Nonlocal but Separable. I. *Phys. Rev.*, 95:1628–1634, 1954.